UNIVERSITY OF HAWAI'I LIBRARY

DETECTION OF HEATBEATS IN WIRELESS SIGNAL

A THESIS SUBMITTED TO THE GRADUATE DIVISION OF THE
UNIVERSITY OF HAWAI'I IN PARTIAL FULFILLMENT
OF THE REQUIREMENTS FOR THE DEGREE OF

MASTER OF SCIENCE

IN

ELECTRICAL ENGINEERING

DECEMBER 2006

By
Qin Zhou

Thesis Committee:

Anders Host-Madsen, Chairperson
Anthony Kuh
Victor M. Lubecke

We certify that we have read this thesis and that, in our opinion, it is satisfactory in scope and quality as a thesis for the degree of Master of Science in ELECTRICAL ENGINEERING.

THESIS COMMITTEE

Chairperson

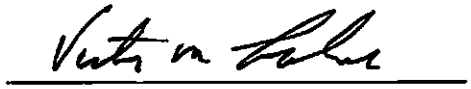

Copyright 2006

by

Qin Zhou

To my mother.

Acknowledgements

There are lots of people I would like to thank for a huge variety of reasons.

Firstly, I would like to express my sincere gratitude to my advisor Professor Host-Madsen, for his guidance and assistance throughout this thesis and my education at the University of Hawaii at Manoa. With his enthusiasm, his inspiration, and his great efforts to teach things clearly and simply, he helped to make research and mathematical derivation fun for me. I really benefit much from the research methodologies and attitude taught by him. I'm also extremely grateful to his prompt help and consideration to study and my life. It is difficult to overstate my gratitude to him.

I'm heartily grateful to Dr. Olga Boric-Lubecke and Dr. Victor M. Lubecke, for their continuous financial support and concern for my research. I wish to thank my committee members, Dr. Victor M. Lubecke and Dr. Anthony Kuh, for giving me many instructions and suggestions to improve my thesis and defense. I'm indebted to Dr. Kuh for his nice advice to my study and future, and heartily grateful to his patience on revising my thesis.

I wish to thank all the rest students of the Doppler radar project. Particular thanks to Byung-Kwon, Shuhei, Dung and Amy, who have cooperated with me to measure and analyze the wireless data. The discussion with them is interesting and inspirational.

Much thanks and great respect to my officemates in POST325: Jianhan, Juntan, Wenyi, Zigui, Yige and Jeff. They have given me generous help and a lot of useful advices, no matter on life or on study. It's a happy and memorable time to work together with them.

I should say a big 'thank-you' to my good friends: Chao, Huilin, Huijuan, Run, Iris and Helen. I really appreciate their warm-hearted encouragement and unwavering spiritual support, especially in my bad days. Hope we can always be good friends.

Lastly, and most importantly, I would like to express special thanks to my parents and sister. They endured this long process with me, always offering support and love. I

want to dedicate this thesis especially to my mother. No matter where is she, I will love her forever.

ABSTRACT

Doppler radar remote detection of heart activity is a promising technique for unobtrusive health monitoring and life sensing. However, so far this approach has been limited to practical use. The difficulty lies in distinguishing targeted heartbeat signals from artifacts produced by the the presence of other people or environmental motion. We are exploring separation of signals from multiple subjects in single and multiple antenna systems. To achieve this objective, the first thing is to detect how many subjects exist in a given area. This thesis mainly focus on design of optimal detectors for this problem. Currently, we are only aim to distinguish among the presence of 2, 1, or 0 subjects with one or two antennas.

For this particular application, the primary concern of a good detector is the selection of an optimality criterion and a good model of the data to statistically describe the principle features. The wireless heartbeat signal due to Doppler shift is a very weak nonstationary signal with time-variant periods. Within each detection window, it is modeled as a sinusoid with constant frequency, but staircase jumpily variant phase and magnitude from subwindow to subwindow. Detection turns into determining how many such sinusoids are present. For detection problem with so many unknown parameters, *General Likelihood Ratio Test (GLRT)* is presented as solution. Although there is no optimality associated with the GLRT, in practice, it appears to work quite well. We have shown that it is possible to distinguish among the presence of 2, 1, or 0 subjects, even with single antenna. The key of success is to find good window structure and length. The detection probability can be improved by using more antennas.

As is well known, GLRT need *Maximum Likelihood Estimation (MLE)* of unknown parameters, especially MLE of the heartbeat frequency. For single person or nobody present cases, MLE of the frequency is equivalent to find the peak of the averaged FFT over subwindows. Based on FFT and GLRT, fast novel heartbeat detection algorithms are presented and evaluated for both real and complex data model. Although real data

model can use SVD combination of multiple antennas to improve performance, complex data model still outperforms the former scheme. Some good window structures are recommended, and their simulation results show that the presented complex detector has a very excellent performance.

Contents

Acknowledgements v

Abstract vii

List of Tables xi

List of Figures xii

1 Introduction 1
- 1.1 History of Doppler radar remote sensing . . . 1
- 1.2 Motivation and schedule of this project . . . 3
- 1.3 RF and baseband signal due to heartbeat . . . 4
- 1.4 Outline of the thesis . . . 8

2 Current Heartbeat Research in Biomedical Signal Processing 11
- 2.1 Introduction of electrocardiogram (ECG) and heart rate variation (HRV) . . . 11
- 2.2 Current research about ECG and HRV . . . 14
  - 2.2.1 The factors that affect heartbeat rate . . . 14
  - 2.2.2 Time domain properties . . . 15
  - 2.2.3 Frequency domain properties . . . 16
- 2.3 Current model for ECG signal analysis . . . 17
- 2.4 Conclusion . . . 18

3 Heartbeat Signal Model 19
- 3.1 Experimental setup . . . 19
- 3.2 Review the wireless and reference signals . . . 20
- 3.3 Basic idea to model heartbeat signal . . . 22
- 3.4 Heartbeat signal model . . . 24
  - 3.4.1 Heartbeat signal model for real data . . . 25
  - 3.4.2 Heartbeat signal model for complex data . . . 26
- 3.5 Conclusion about heartbeat signal model . . . 27

4 Detection of Heartbeats 29
4.1 Methods to detect the number of sinusoids 29
4.2 Neyman-Pearson (NP) test and GLRT 30
4.3 MLE of unknown sinusoids 31
4.4 Detection of heartbeats by GLRT 33
4.4.1 GLRT with single channel 33
4.4.2 Extension to multiple channels 34
4.5 Data requirement to be successfully detected 34
4.5.1 GLRT detection results with single channel 36
4.5.2 Conclusions about detection 39

5 SVD Combination to Improve the SNR 42
5.1 Difficulties in extracting heartbeat from IQ data 42
5.2 Introduction to Singular Value Decomposition (SVD) 45
5.3 Maximum likelihood identification of a signal subspace by SVD 46
5.4 Enhance SNR with SVD-combination 47

6 Fast FFT-GLRT-based Detection 52
6.1 Detection for real data model 52
6.1.1 GLRT and MLE of parameters when noise is unknown 52
6.1.2 GLRT and MLE of parameters when noise is known 56
6.2 Detection for complex data model 57
6.3 Detection performance analysis 63
6.3.1 Definition of P_A, P_D and ROC 63
6.3.2 Apply thresholds and get P_D for a given P_{FA} 64
6.3.3 Simulation results and ROC curves 64

7 Further Research Ideas 73

8 Conclusions 75

Bibliography 78

List of Tables

List of Figures

1.1 A single antenna system with single subject. 2

2.1 Sensitive electrodes are placed on certain parts of the body to get ECG . . . 12
2.2 ECG waveform segment model 13
2.3 Normal ECG Curve and RR interval 13
2.4 Heartbeat signal in time domain (by finger sensor) 15
2.5 Heartbeat signal in frequency domain (by finger sensor) 16

3.1 Photograph of an Experimental Doppler radar set-up 20
3.2 filtered wireless and reference signal in frequency domain. 21
3.3 filtered wireless and reference signal in time domain. 22
3.4 Heartbeat Signal Model 26

4.1 Good test result. Top: GLRT, 2 or < 2 subjects. Bottom: GLRT: 1 or 0 subject 36
4.2 IQ constellation of Good test result 37
4.3 Bad test result. Top: GLRT, 2 or < 2 subjects. Bottom: GLRT: 1 or 0 subject 38
4.4 IQ constellation of Good test result 38
4.5 Comparison: GLRT for 2/1/0 person with single antenna 39
4.6 Comparison: GLRT for 2/1/0 person with 2 antennas 40
4.7 Comparison: GLRT for 2/1/0 person with 4 antennas 40

5.1 The IQ constellation for received data with high SNR 43
5.2 The IQ constellation for received data with low SNR 44
5.3 Comparison: PSD of 4 channels data 49
5.4 Comparison: PSD of SVD-combined data 50
5.5 Comparison: SVD-combined data and complex data in time domain 51

6.1 Read data model with SVD combination, P_D under a given P_{FA}, window = 24s 65
6.2 Reference data, P_D under a given P_{FA}, window = 24s 65
6.3 ROC: Simulation for window=24s, real model with SVD combination . . . 68
6.4 ROC: Simulation for window=32s, real model with SVD combination . . . 69

6.5 ROCs for real model with SVD combination versus different parameters . . 69
6.6 ROCs of Antenna 2 for complex model versus different parameters 70
6.7 ROCs of Antenna 1 for complex model versus different parameters 70
6.8 ROC comparison: real model (SVD) versus complex model, antenna 2 . . 71
6.9 ROC comparison: real model (SVD) versus complex model, antenna 1 . . 71
6.10 ROC comparison for complex model: antenna 2 versus antenna 1 72
6.11 IQ Plot of noise at 2 antennas 72

Chapter 1

Introduction

1.1 History of Doppler radar remote sensing

With the advances in technology and improvement of life quality, health attracts more and more concern. At the same time, due to the increasing population of elderly and chronic patients world wide, there is a big market for cheap, all time available post-hospital patient home care and health monitoring techniques. This requires appliances that provide a scheme that can monitor health parameters outside of the traditional hospital environment and efficiently transfer data to doctors. Such appliances could provide continuous monitoring, avoid disturbing a subject's physiological and/or emotional state, make the untouchable measurement realizable, reduce pain or uncomfortableness of patients, and cut the overall health care cost . Particularly in special circumstances, it has a clear advantage that it can offer a reliable monitoring scheme when direct touch with subjects is limited or impossible.

Based on microwave Doppler principle, wireless communications technology can provide a platform for above monitoring[2] [3]. The basic theory of Doppler radar is illustrated in Fig.1.1. A homodyne radio is used to detect the phase shift proportional to chest displacement due to cardiopulmonary activity. By the Doppler effect, an RF wave reflected

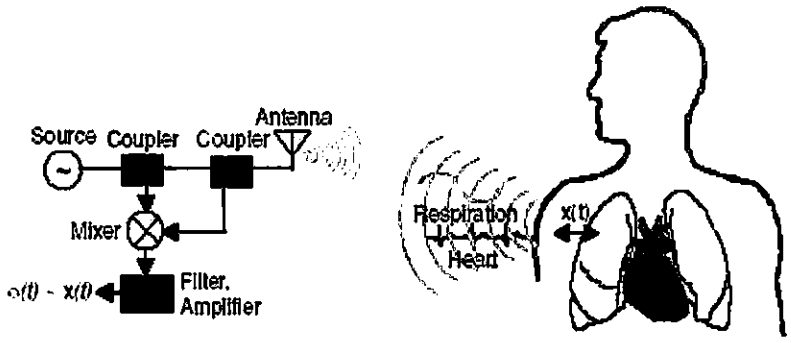

Figure 1.1: A single antenna system with single subject.

at a moving surface undergoes a frequency shift proportional to the surface velocity. If the surface is moving periodically, such as the chest of person breathing, this can be characterized as a phase shift proportional to the surface displacement. If the movement is small compared to the wavelength, a circuit that couples both the transmitted and reflected waves to a mixer can produce an output signal with a low-frequency component that is directly proportional to the movement. This is the case when measuring chest surface motion related to respiration and heart activity. Internal body reflections are greatly attenuated (more severely with increasing frequency) and will not be considered. From the output signals of antennas, we can detect and locate subjects with signal processing techniques.

Detection of heart and respiration with Doppler radar was first demonstrated in the 1970's by using X-band waveguide transceivers [4][5][9]. Due to expensive RF components, it wasn't widely used. However, today's booming wireless communication technology and IC design industry have produced widely available cheap hardware and software components. Doppler radar now can be implemented with inexpensive radios or wireless communication devices. Therefore, Doppler radar was rediscovered recently for the purpose of health monitoring and life sensing [6]. Together with the broad band wireless

network, the received data can be transferred to health care professionals or any monitoring centers for particular purpose. Benefit from Doppler radar remote sensing, long distance diagnostician and health care can really be implemented and widely used.

Furthermore, Doppler radar remote detection of vital signs and activity also has a lot of other applications. For example, it can be used to find survivors in disaster situations like earthquakes, or be used for military recognizance. In a word, this technique is so useful, having significant applications in many different areas.

1.2 Motivation and schedule of this project

Although microwave Doppler radar sensing has shown to be promising, it has not fit practical applications in remote subject detection. The difficulty lies in distinguishing targeted heartbeat and respiration signals from artifacts produced by the presence of other people or environmental motion. So far this approach has been limited to sensing and detection of a single subject, and the detection probability is not desirable. When there are two or more subjects in view, it is more challenging to isolate signals from individual subjects.

We are exploring separation of signals from multiple subjects in single and multiple antenna systems. In a single antenna system, based on expected different spectral signatures of individual cardiovascular related motion, it is possible to separate individual signals in frequency domain. In a multiple antenna system (SIMO or MIMO), even if individual cardiovascular signatures are very similar, it is possible to distinguish different subjects based on angle of arrival. In this paper, the theoretical background and experiment results for both of these approaches will both be discussed.

The idea of employing MIMO systems to enhance the quality of signals received by Doppler radar, is inspired by its powerful function in wireless communication system. Instead of distortion by multipath, MIMO systems can exploit multipath to dramatically

enhance wireless channel capacity and increase the transmission accuracy. When only a single source (or person) exists, MIMO system can increase the output SNR and combat interference. When multiple sources show up, MIMO can isolate information of different individuals with blind source separation (BSS) technique [33]. We believe that advances could be made for this technology through a research effort and the current bottleneck problems can be overcome. In spite of all the difficulties, we are headed in the right way toward the goal.

The whole project is divided into several phases. In the first phase, the objective is to determine how many targets exist and where they are in a given area. In this phase, we only consider still targets, and use 1 antenna as the transmitter, but 1 or 2 antennas as the receiver. For the long-term goal, we want to detect and track subjects in movement, and to separate information of different targets. Finally, we hope the detected information of subjects can satisfy the requirement of remote monitoring, and finally apply this technique to long distance health care.

Currently the project is in the first phase. This paper mainly focuses on the detection of the number of subjects(2/1/0) within range of the antennas, and possibly location through direction of arrival (DOA). The result can be used to post-disaster rescues and military recognizance.

1.3 RF and baseband signal due to heartbeat

To solve a detection problem, first of all, we must know well about the received RF and baseband signal. We assume a continuous wave (CW) radar system transmits a single tone signal at frequency ω. This signal is reflected from a target at a nominal distance d, with a time-varying displacement given by $x(t)$. Suppose at first that the signal from a given subject arrives from a single path. The sampled, passband received signal at the n-th

antenna in a SIMO system with quadrature receivers can be written as

$$\begin{aligned} r_n(t) &= A\exp\{j[\omega(t+x(t-n\phi)-n\phi)+\varphi]\}+w_n(t) \\ \phi &= \frac{d}{c}\sin(v) \end{aligned} \tag{1.3.1}$$

where A is determined by the power reflection factor; φ is the basic delay between transmission and receiving, decided by the distance between the subject and the $0th$ sensor in the array; $n\tau$ is the nth sensor's additional delay due to its position. Here t is of the order $1/(3\cdot 10^8)$, so that $x(t-n\phi)\approx x(t)$. After down frequency conversion, the baseband-received signal can be written as

$$\begin{aligned} r_n(t) &= A\exp\{j[\omega(t+x(t)-n\phi)+\varphi]\}+w_n(t), n=0,\ldots,M-1 \\ \phi &= \frac{2\pi d}{\lambda}\sin(v) \end{aligned} \tag{1.3.2}$$

for a linear array, with angle of incidence v and noise $w_n(t)$. If we collect the signal received at the M antennas into a vector, this can be written as

$$\begin{aligned} \mathbf{r}(t) &= Ae^{j\varphi}\exp(j\omega x(t))\mathbf{s}(\phi)+\mathbf{w}(t) \\ \mathbf{s}(\phi) &= [1,\exp(j\phi),\ldots,\exp(j(M-1)\phi)]^T \end{aligned} \tag{1.3.3}$$

As $\omega x(t)$ is very small

$$\exp(j\omega x(t))\approx(1+j\omega x(t)) \tag{1.3.4}$$

is a good linear approximation, so that

$$\mathbf{r}(t)\approx Ae^{j\varphi}(1+j\omega x(t))\mathbf{s}+\mathbf{w}(t) \tag{1.3.5}$$

Thus, the signal is characterized by a characteristic vector s. If there are now S subjects at different positions, they will likely have different DOA vectors s, and we can write the total received signal as

$$\begin{aligned} \mathbf{r}(t) &= \sum_{s=1}^{S} A_s e^{j\varphi_s}\exp(j\omega x_s(t))\mathbf{s}_s+\mathbf{b}+\mathbf{w}(t) \\ &\approx \sum_{s=1}^{S} j\omega A_s e^{j\varphi_s}x_s(t)\mathbf{s}_s+\sum_{s=1}^{S} A_s e^{j\varphi_s}\mathbf{s}_s+\mathbf{b}+\mathbf{w}(t) \end{aligned} \tag{1.3.6}$$

where b is a DC component due to reflection from other objects (e.g., walls, furniture) than humans. If we use the approximation Eq.1.3.4we then get Eq.1.3.6.

In the following text, we only consider the signal $A_s x_s(t)\mathbf{s}_s$. If IQ channels are both available,A_s is complex; otherwise, for single channel I or Q, A_s is real. When there are multiple antennas,$\mathbf{s}_s$ contains the DOA ϕ. However, for single antenna case, the received baseband signal degrades into $A_s x_s(t)$, and can be abbreviated as $x_s(t)$.

As to the baseband signal model, there are several points needed attention:

Baseband IQ and DC component If we consider individual subject, for each subject, we can combine ϕ into φ, that means the total delay between transmitter and receiver due to a single subject. The measured I and Q data are given by:

$$\begin{aligned} I &= Re\{Ae^{j\varphi}(1 + j\omega x(t)) + w(t)\} \\ &\approx A\cos(\varphi) - A\sin(\varphi)\omega x(t) + Re\{w(t)\} \\ Q &= Im\{Ae^{j\varphi}(1 + j\omega x(t)) + w(t)\} \\ &\approx A\sin(\varphi) - A\cos(\varphi)\omega x(t) + Im\{w(t)\} \end{aligned} \tag{1.3.7}$$

in which A is power attenuation due to reflection; ω is the carrier frequency; φ is unknown, determined by the distance and DOA between the subject and the antenna; w(t) is WGN. Only x(t) contain heartbeat information. Only φ contains position information. I and Q have different DC and magnitude. These factors depend on the subject's position.

Although each subject cause a DC component, there are other DC components due to reflection and hardware problem. All DC components mix up together, and it's hard to get useful information from DC, thus, for simplicity, we give up and remove all the DC component.

Coefficients of signal x(t): A, φ, ω Since currently we only study the still subjects, φ should be constant during measurement. If we combine it into magnitude A, the factor

$exp(j\varphi)$ disappears, but different subjects will have different value A. For frequency ω, we assume it's constant within a detection window.

Removal of respiration It's deserved to notice that, any motion can cause displacement. So we require the subjects keep still and don't speak during measurements. But respiration due to chest movement can't be prohibited. Therefore, the baseband signal $x(t)$ generated by each subject consists of respiration and heartbeat. Fortunately, heartbeat and respiration has different frequency range. The respiration is usually in the range $0 - 0.8$Hz and the heartbeat in the range $0.8 - 2$Hz. While the respiration is a stronger signal than the heartbeat, it is also more difficult to characterize and therefore to detect. We just utilize a very sharp bandpass filter with the same band of heartbeat frequency range, to remove all the respiration and interferences, and totally remove all the DC minus the mean of data.

Multiple receiving antennas and diversity gain The subject's position cause different magnitudes for Q and I. In the worst case, very bad position and DOA would cause one magnitude degrade to 0, the heartbeat information in one channel will be canceled. For safety, sometimes we use 2 antennas to provide multiple versions of wireless heartbeat signals. If we do that, we will get diversity gain, then by smartly combination of different channels' data, we can increase the SNR and obtain better detection performance. These ideas are widely used in MIMO techniques.

Record signal with finger sensor for reference We not only measured wireless data, but also record the data by finger sensor for reference. The finger sensor works just like electrocardiogram. It can offer us a very clear signal about heartbeat. Although the finger sensor and Doppler radar works with different theories, their resulting data records contain similar information, particularly in terms of the main frequency. This will be shown in Chapter 2. All this provide important clues to model the heartbeat signal.

Therefore, we can observe reference signal to build up heartbeat signal model. By the way, although heartbeat is widely and deeply researched in medcine and cardiovascular field, the popular models in these fields don't fit our purpose of signal processing and detection. However, they provide some useful information. The most important one is that, it's a nonstationary, nearly periodic, but the period varies with time. We can observe that, for small engouh interval, the heartbeat signal can be treat a sinusoid signal. In long time view, it can be treat as a sinusoid with time varying magnitude and phase. Therefore, the heartbeat can be modeled as time-varying sinusoid, the residual heart variation can be combined into noise. The noise can be treated as white Gaussian with unknown variance.

1.4 Outline of the thesis

In this thesis, heartbeat signal models and algorithms to detect the number of subjects in view are presented and evaluated. Aimed for better performance and simpler hardware implementation, a new phase jumping heartbeat model, and a novel detection algorithm based on FFT and GLRT, are presented and evaluated.

In Chapter 2, the current research about heartbeat in biomedical signal processing field based on Electrocardiogram (ECG) observation by direct contact sensors is introduced. Despite difference from Doppler radar measurements, the ECG record contains similar heartbeat information. Its basic concepts and theories are illustrated. Although the existing hearbeat models are not fitting for detection purpose, research results in this field show us that heartbeat is a nonstationary signal with time-variant periods.

Taking advantage of the heartbeat characteristic depicted in chapter 2, I present my own heartbeat model in Chapter 3. Within each detection window, heartbeat is modeled as a sinusoid with constant frequency, but staircase jumpily variant phase and magnitude (per subwindow). The residual heartbeat variation is combined into noise, which is assumed to be white Gaussian. For complex wireless signal, since heartbeat information em-

bedded in both I and Q channel, we can exploit real or complex data to detect. Therefore, both real and complex data models are illustrated.

The detection problem is discussed in Chapter 4. With the purpose to determine the number of subjects (0/1/2) with single antenna, for simplification, we prefer to state the problem as a traditional Neymann-Pearson hypothesis test. Since the frequency and phase of each subject are unknown and variant with time, and the noise parameters is also unknown, it is a composite detection problem with many unknown parameters and no Uniform Most Powerful(UMP) test exists. The best detector for this kind of problem is commonly accepted to be the generalized likelihood ratio test (GLRT). Some good and bad detection results are shown as examples, and what kind of data can be correctly detected is described.

SNR is a critical factor for detection performance. Under low SNR many ordinarily good detectors don't work well any more. For real data model, to enhance the received data's SNR, in Chapter 5, *Singular Value Decomposition* (SVD) combination is presented. Under the theory of Principle Component Analysis (PCA), the combined data would capture the most significant component of the data, and consequently result better detection performance.

Furthermore, we suspect that the improper signal model attributes to the abnormal SNR. For further improvement, in Chapter 6, some modification about heartbeat model is made and an almost harmonic model with constant frequency jumping phase is described. For single target case, the algorithm for Maximum likelihood estimate of unknown parameters is derived, and applied to GLRT. It results that FFT is used in analytically searching for MLE of heartbeat frequency. ROC curves obtained by simulation show that, for hypothesis test of 1/0 target, this novel proposal provides higher detection probability and much faster speed than the GLRT of old model in Chapter 3 . In addition, for 2-target case, we can utilize blind source separation method like Constant Modulus Algorithm (CMA) to split

composite information into individuals' first, then use this proposal to determine whether there are 2 targets or not.

As is well known, GLRT need *Maximum Likelihood Estimation (MLE)* of unknown parameters, especially MLE of the heartbeat frequency. For single person or nobody present cases, MLE of the frequency can be simplified by searching the peak of the averaged FFT over subwindows. In chapter 6, fast novel heartbeat detection algorithms based on FFT and GLRT are presented and evaluated for both real and complex data model. Although real data model can use SVD combination of multiple antennas to improve performance, complex data model still outperforms the former scheme. Some good window structures are recommended, and their simulation results show that the presented complex detector has a very excellent performance.

In chapter 7, further ideas about 2-target detection and location are discussed. We can exploit blind source separation method like Constant Modulus Algorithm (CMA) to split composite information into individuals' first, then the FFT-GLRT-based single person detection method can be used to determine whether there are 2 targets or not. Another promising method is ROOT-MUSIC algorithm, which is a high-resolution signal parameter estimation algorithm, particularly at low SNR. ROOT-MUSIC algorithm can provides information about the number of incident signals, Direction-Of-Arrival (DOA) of each signal, strengths and cross correlation between incident signals, noise power, etc. However, it requires very precise and accurate array calibration.

Finally, some conclusions about the main contributions of this thesis are given in Chapter 8.

Chapter 2

Current Heartbeat Research in Biomedical Signal Processing

2.1 Introduction of electrocardiogram (ECG) and heart rate variation (HRV)

At the mention of heartbeat research, many people instantly associate it with the Electrocardiogram (ECG). ECG is a recording of the small electric waves being generated during heart activity, which shows the rate and regularity of heartbeats. It is world widely used today as a relatively simple way of diagnosing heart conditions.

Although the basic theories behind ECG and Doppler radar remote sensing are different, under small or moderate noise, the heart beat frequencies measured by these two methods are very close. It can be verified in spectrum that peaks show up at the same frequency within the range of heartbeat, with the peaks corresponding to the heart beat frequency. In this research, when measuring the wireless signal by Doppler radar, we also use a finger strap sensor to record signals for reference. The finger strap sensor works similar to ECG. This reference signal contain clear information about heartbeat, and can help to evaluate the wireless signals, or to troubleshoot problems in remote measurements.

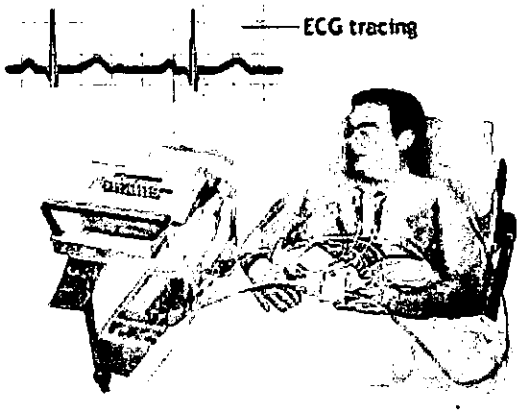

Figure 2.1: Sensitive electrodes are placed on certain parts of the body to get ECG

Hence, we'll review current research in the field of ECG. Some models or useful properties of heartbeat in this field are cited. Although the existing models are not fit for detection purposes, the heart beat properties let us be aware of difficulties in detection or estimation of multiple targets.

Let's first give an introduction to ECG and its extended analysis – heart rate variation (**HRV**). A normal ECG curve looks like Fig.2.2, which contains 5 different waves [30]: P Q R S T. **P-wave** is produced by muscle contraction of atria. **R-wave** marks the ending of atrial contraction and the beginning of ventricular contraction. Finally, T-wave marks the ending of ventricular contraction. The magnitude of the R-wave normally ranges from 0.1 mV to 1.5 mV. A narrow and high **R-wave** indicates a physically strong heart. The signal between two continuous R-wave is named as **R-R interval**. R-R interval is usually used to measure the period of heartbeat, because it should be relatively constant from beat to beat. Fig.2.3 shows two complete cycles of a normal ECG waveform. The inverse of R-R interval is the **heart rate**. A changing R-R interval indicates irregular heart rate. The changes of beat-to-beat fluctuations in heart rate have been called **heart rate variability**. Under resting conditions, the ECG of healthy individuals exhibits periodic variation in R-

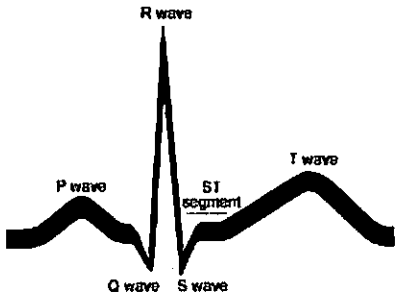

Figure 2.2: ECG waveform segment model

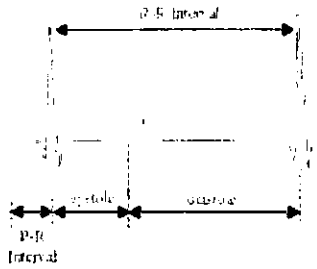

Figure 2.3: Normal ECG Curve and RR interval

R intervals. The analysis of heart rate variability has been used as a non-invasive tool to assess cardiovascular autonomic regulation of the heart. The reasons why we can use ECG to monitor health condition is that: with further analysis tools like Lorenz plot(or Poincare Plot) and so on, or by checking the HRV, most slight pathologic changes can be revealed. Thus doctors can easily diagnose the corresponding illness but with a very high success ratio. Besides determining the presence of any damage to the heart, by use of ECG, we can also easily evaluate the effects of drugs or devices used to regulate the heart.

The apparently easy derivation of ECG and HRV measures has popularized their use. And most commercial devices now provide automated measurement of HRV. It is a simple, cheap but very useful tool for both research and clinical studies.

2.2 Current research about ECG and HRV

In recent research in cardiovascular field, heart rate variability (HRV)is a cut-edging topic. The European Society of Cardiology and The North American Society of Pacing and Electrophysiology constituted a Task Force, which was charged with the responsibility of developing appropriate standards of measurement, physiological interpretation, and clinical use for HRV. A standard document[11]was presented by this Task Force in 1996, in which many properties of HRV are illustrated and some research methodologies are recommended.

HRV has received much more attention than the heart rate itself. However, in the view of digital signal processing, we are more interested in heatbeat **instantaneous frequency**, and their statistic properties in time domain, frequency domain, or even time-frequency domain. It's really a very important thing if we want to set up a model of heartbeat, particularly for detection or estimation purposes.

It's obviously that instant heart rate changes attribute to the HRV. Although existing documents didn't cover much about the instant heart rate, they can still offer us useful information in many aspects. These are helpful to get a picture of what heartbeat signal looks like. They can provide a friendly reminder of what we should pay attention to and what we needn't waste time on.

2.2.1 The factors that affect heartbeat rate

All time and frequency domain measures of HR variability could be affected by artifacts and ectopic beats. Heartbeat is also highly related with the subject's health condition. Even the ordinary motion like eating, laughing, talking can cause heart rate changes a lot. Research shows that the heart rate increases and the variance becomes large during an ictal event, and they decrease back towards a normal range after the ictus event.

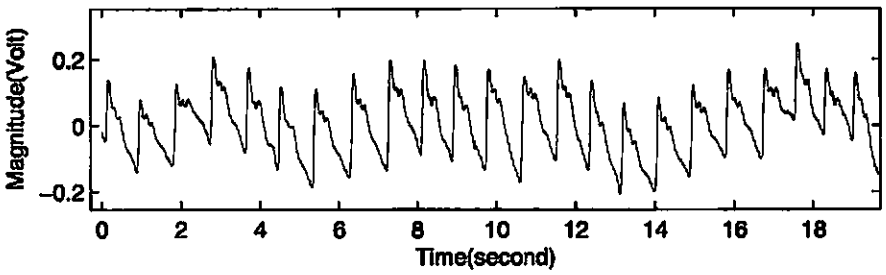

Figure 2.4: Heartbeat signal in time domain (by finger sensor)

During the non-ictal activity heart rate is stable and has less variation [10]. Besides these, HRV is also affected by psychosocial factors, age, and population, etc.

The following results are got under the hypothesis that these artifacts and ectopic beats have been eliminated. The subjects are healthy and don't move during measurement.

2.2.2 Time domain properties

The time domain measures of heart rate variability are calculated by statistical analysis (means and variance) from the lengths of successive R-R intervals. R-R intervals fluctuate in a complex, apparently erratic manner in healthy subjects even at rest. The most commonly used time domain indexes are the average heart rate and the standard deviation of the average successive R-R intervals calculated over a 24-hour period. There are also other time-domain measures of HR variability. But so far, experimental and simulation data appear to indicate that the various methods of expressing HRV are largely equivalent, and there is no evidence that any one method is superior to another, provided measurement windows are 5 minutes or longer [11]. Because of this, in measurements we always record data as long as 5 minutes.

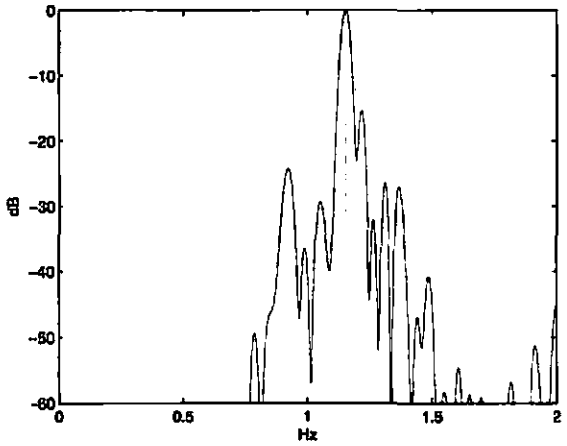

Figure 2.5: Heartbeat signal in frequency domain (by finger sensor)

2.2.3 Frequency domain properties

A normal heartbeat frequency range is $0.8 \sim 2$Hz. Fig.2.5 shows the FFT of heartbeat signal produced by finger sensor, with a length of 48 second data. The corresponding frequency at the peak means the average instantaneous frequency in this interval. The most popular research about heart rate is developed by counting RR intervals, and by studying spectral characteristics of heart rate variability.

Analysis of heart rate variability mainly focused on short time oscillations associated with breathing ($0.15 \sim 0.40$Hz) and blood pressure control ($0 \sim 0.10$Hz) [15]. Examination of 24-hour Heart Rate records indicates Heart Rate is nonstationary and exhibits a $1/f^{\alpha}$-type spectrum [15][13]. In addition, α varies with time scale and is different for normal ($\alpha \approx 1$) and congestive heart failure ($\alpha \approx 1.5$) subjects. Simulations suggest that a possible mechanism underlying the observed power-law spectrum may be a switching between values of α near zero (white noise) and near two (Brownian motion).

The spectral analysis of HR variability gives a possibility to study the frequency-specific fluctuations of heart rate[16]. The power spectrum reflects the amplitude of heart

rate fluctuations present at different oscillation frequencies. Paper [14] compares Fourier, autoregressive, and Lomb power spectral density(PSD) estimates from synthetic, real, and noise-corrupted real heart rate time series, and examines systematic differences among these estimates. And a good algorithm is presented for obtaining a heart rate time series suitable for Lomb PSD estimation from an RR interval time series.

2.3 Current model for ECG signal analysis

The HRV signal is commonly modeled by an integral pulse frequency modulation (IPFM) scheme. The integral pulse frequency modulation (IPFM) model converts a continuous-time signal into a modulated series of event times, often represented as a pulse train. The IPFM process is important to the field of heart rate variability (HRV) as a simple model of the sinus modulation of heart rate. Based on the model, several techniques have been proposed in the literature to capture features of the HRV signal [16] [17].

A dynamical model based on three-coupled ordinary differential equations is introduced by McSharry in [18], which is capable of generating realistic synthetic electrocardiogram (ECG) signals. The dynamical equations of motion are given by a set of three ordinary differential equations. The operator can specify the mean and standard deviation of the heart rate, the morphology of the PQRST cycle and the power spectrum of the RR tachogram. This model may be employed to assess biomedical signal processing techniques, which are used to compute clinical statistics from the ECG.

However, these two models are too complex and impractical for purpose of detection and estimation. To simplify the problem, according to heartbeat characteristics, we formulate our own model.

2.4 Conclusion

Current research about heartbeat in the field of cardiovascular mostly focus to ECG and HRV. In measurements, artifacts, ectopic beats, and background noise might contaminate the heartbeat signals. Often the level of contamination is such that heartbeat signals are completely hidden by these unwanted signal components. Except for these factors, the health condition and movement of subjects can also affect the heart beat frequency.

It is revealed that heartbeat is a nonstationary time-variant signal, which sets up rather adverse conditions for heartbeat measurement and signal processing. Even if subjects don't move and there is no noise and interference, heartbeat is still a nonstationary signal, and heart rate(instantaneous frequency)is also time-varying in the range of $0.8 \sim$ 2Hz. Fourier analysis of heart rate variability for long heart rate data sets from healthy individuals typically reveals a $1/f$-like spectrum. However, to best capture the short-term characteristics of heartbeat, long record length is helpless, and the suggested record length is 5 minutes.

The existed models mostly consider the heartbeat as IPMF or dynamic procedure. However, these models are not fitting for purposes of detection and estimation. We must design a model, which not only can describe the dominant properties of heartbeat, but is also suitable for a simple effective detector and estimator. Furthermore, the presented model must assure that under normal conditions, most measured data have reasonable high SNR. Otherwise, unfitting model will cause resulting SNR too low, and lead to detection and estimation become very difficult, even having no satisfactory solution.

Chapter 3

Heartbeat Signal Model

The choice of a good detector for a particular application depends on many considerations. Primary concern is the selection of an optimality criterion and a good model for describing the data statistically. The data model should be complex enough to describe the principle features of the data, but at the same time simple enough to allow for optimal detectors and easy implementation[19].

For heartbeat detection, the most important thing is to select a good enough signal model, then if possible, try to find an optimal detector for the presented signal model, otherwise, turn to suboptimal but still excellent detectors.

Chapter 3, 4, and 5 will mainly focus on the above problems. Chapter 3 formulates my own heartbeat signal model. Chapter 4 illustrate its corresponding detector design. Since the detection is a composite problem, generally, we use Generalized Likelihood Ratio Test (GLRT). Although GLRT can't assure optimality, in most cases it works well.

3.1 Experimental setup

Let's first see the typical measurement setup with Doppler radar. A single antenna system, with one subject in the antenna field of view, is illustrated in Fig.3.1.One antenna as transmitter, two antennas as receiver; they are fixed horizontally. A single subject sits

Figure 3.1: Photograph of an Experimental Doppler radar set-up

about 0.5 meters in front of the antennas. Generally, DOA is very small, only about 0-30 degree. For 2 subjects case, 2 persons will sit there side by side. The lab is shielded from all RF interferences. Before tests, all other people except of subjects must get out of the lab. We measured wireless data, and also the data by finger sensor for reference.

The return signal is mixed with a sample of the transmitted signal to produce an output voltage with its magnitude proportional to the phase shift between them, which in turn is proportional to chest displacement due to cardiopulmonary activity. All radar measurements were conducted with the CW signal source at 2.4GHz with 0dBm output power.

3.2 Review the wireless and reference signals

Let's observe the received data in time domain and frequency domain. Fig.3.2 shows a typical heart beat signal, compared with a reference signal measuring the pulse from a finger sensor. The signal has been filtered with a bandpass filter with band 0.8-2Hz.

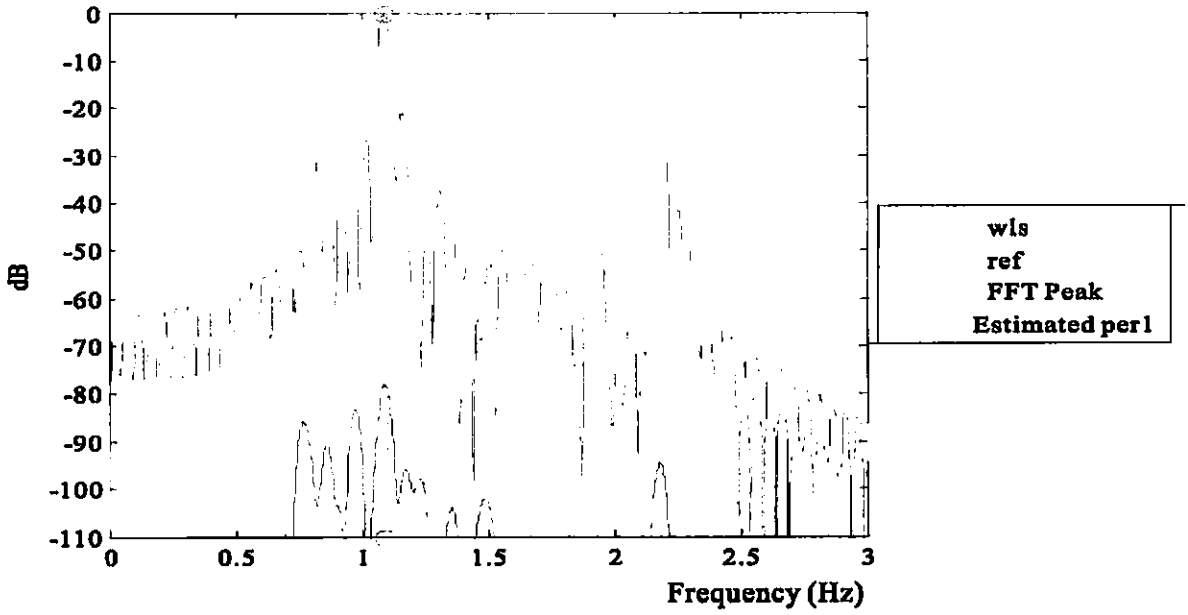

Figure 3.2: filtered wireless and reference signal in frequency domain.

The respiration and all the other frequency content beyond heartbeat range are already removed. The blue curve is the inphase channel data of wireless signal, the red curve is the reference signal produced by finger sensor. We do FFT with 20s long data. In frequency domain, we can see, the wireless and reference signal has similar spectrum, and show peaks almost at the same frequency, which is exactly the heart frequency. This proves that the two kinds of data contains similar information, especially the same main frequency component. This also means our measurement with Doppler radar is successful.

Fig.3.3 shows these two signals in time domain. From the figure, we can see three things: Firstly, the wireless signal, compared with the reference signal, is very noisy, and the heartbeat cannot be found simply from peak detection. Secondly, the heartbeat signal is very weak. Although magnified by 10 times, it's still very small in comparison with the reference signal. This verifies our linear approximation of $\exp(j\omega x(t)) \approx (1 + j\omega x(t))$ in Chapter 1 is correct. Thirdly, for small enough interval, the heartbeat signal can be

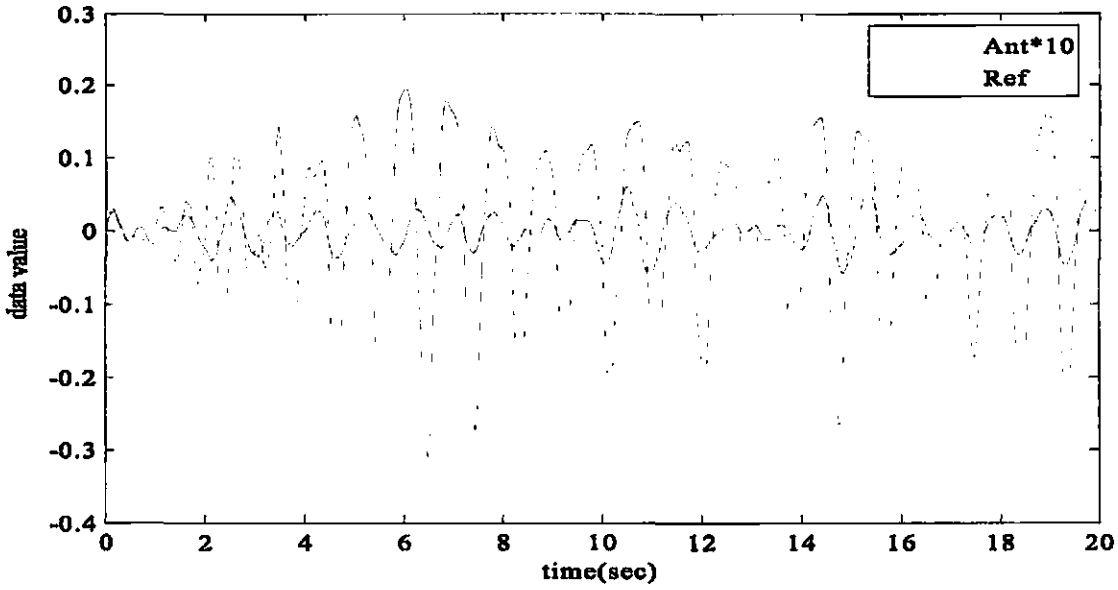

Figure 3.3: filtered wireless and reference signal in time domain.

treat a sinusoid signal. In a long time view, it can be treat as a sinusoid with time varying magnitude and phase. All the characteristics observed in time and frequency domains provide important clues to formulate a model for the heartbeat signal.

3.3 Basic idea to model heartbeat signal

The heartbeat signal is a rather complicated signal. It is nearly periodic, but the period can vary from one beat to the next; this is called heart rate variability (HRV). In Chapter 2, we know HRV can be modeled as a nonstationary random process with strong periodicity, but the period varies with time. We filter the received signal with a bandpass filter with a pass band of 0.8-2Hz so that only the fundamental frequency of the heartbeat is received. Basing on these, and together with our observance in time and frequency

domains, we can see, the heartbeat can be modeled as a time-varying sinusoid, and the residual heart variation can be combined into noise.

In short term, for the ith subject, the resulting heartbeat signal(channel I or Q) is modeled as

$$\begin{aligned} x_i(t) &= [A_i + \alpha_i(t)]\cos[\omega_i t + \phi_i(t) + \theta] \\ &= A_i \cos(\omega_i t + \theta) + w(t) \end{aligned} \tag{3.3.1}$$

$$\begin{aligned} w(t) = \quad & A_i[\cos(\phi_i(t)) - 1]\cos(\omega_i t + \theta) \\ & + \alpha_i(t)\cos[\omega_i t + \phi_i(t) + \theta] \\ & + [A_i + \alpha_i(t)]\sin(\omega_i t + \theta)\sin(\phi_i(t)) \end{aligned} \tag{3.3.2}$$

Notice that, we combine the DOA effect into magnitude $A_i + \alpha_i(t)$.The amplitude variations $\alpha_i(t)$ and $\phi_i(t)$ are zero mean random processes modeling the HRV. We assume that these have zero mean not only at DC but also at all frequencies, i.e.,

$$\lim_{T\to\infty} \frac{1}{T}\int_{-T}^{T} \alpha_i(t)e^{-i\omega t}dt = \lim_{T\to\infty} \frac{1}{T}\int_{-T}^{T} \phi_i(t)e^{-i\omega t}dt = 0$$

From this we can conclude that

$$\lim_{T\to\infty} \int_{-T}^{T} w(t)e^{-i\omega t}dt = 0$$

and therefore that

$$\lim_{T\to\infty} \int_{-T}^{T} x_i(t)e^{-i\omega t}dt = \begin{cases} 1 & \text{if } \omega = \omega_i \\ 0 & \text{if } \omega \neq \omega_i \end{cases}$$

Thus, if we calculate the Fourier transform (and not the power spectral density) of the received signal, we can expect to see peaks at the heartbeat frequencies ω_i. The HRV is included in the term $w(t)$ which can be seen as an additional noise term. We assume the noise $w(t)$ is zero mean white Gaussian with unknown variance. Since $w(t)$ includes terms due to HRV, the assumption that it's WGN is indeed a rough approximation. However, in absence of detailed information about HRV terms, one can argue from maximum entropy principles that a WGN model is the most robust.

3.4 Heartbeat signal model

In a short interval, we know the filtered wireless signal may be coarsely approximated as a sinusoid whose instant frequency frequency and amplitude still can be treated as fixed. But in a long run, the model is slightly different. We think the frequency and amplitude slightly change. We want to set up a model, which can be applied to all the data no matter in a short term or in a long term.

A satisfactory model is presented in this section. Since we proceed detection window by window, to consider heartbeat variation(HRV), we divide a window into M subwindows, each with the same length N. For each subwindow, the magnitude and phase remain constant, but they jumpily change subwindow by subwindow.

The presented model is illustrated with mathematics in the following text. As a rationale, the frequency variance is equivalent to phase shift. For the purpose of single tone detection, we prefer to keep the frequency constant to obtain the convenience in determine if there is a single tone exists or not. Assume T is the sampling period. For a certain length of heartbeat samples, we can accurately model the heartbeat as a single constant frequency signal with phase shift like this:

- We count a length of MN samples as an interval. For each interval, the frequency is constant, but amplitude and phase are variant
- Each subinterval has N samples. Within the subinterval, the frequency, amplitude and phase are all constant
- From subinterval to subinterval, the frequency remains the same, whereas amplitude and phase has staircase jumping
- For each subinterval, the amplitude and phase are independent of each other. Furthermore, they are also independent of the samples before or after the current interval. It can be treated as a cause system, and without memory

- The frequency jumpily changes from interval to interval (with length MN)
- Assume the noise is independent Gaussian noise with variance σ^2

No matter the record data is real or complex, the signal by heartbeat Doppler shift is all along like a sinusoid, only the magnitude of the data changes between real and complex. Then the measurement taken at the nth sample of the mth subwindow can be expressed as

$$s_m[n] = A_m \cos(wt_{mn} + \theta_m) \tag{3.4.1}$$

$$m = 0, \ldots, M-1 \qquad and \qquad n = 0, \ldots, N-1$$

When the record data is real, A_m is real; when the record data is complex, A_m is complex. With our assumption, $A_0, A_1, \ldots, A_{M-1}$ are different and independent real data;$\theta_0, \theta_1, \ldots, \theta_{M-1}$ are also different and independent.

3.4.1 Heartbeat signal model for real data

Let's first consider the case that the record data is real. To avoid the nonlinearity estimation of parameters inside cos, we substitute A_m and θ_m with another two coefficients a_m and b_m:

$$s_m[n] = A_m \cos(wt_{mn} + \theta_m) = a_m \cos(\omega t_{mn}) + b_m \sin(\omega t_{mn}) \tag{3.4.2}$$

in which $(a_0, \ldots, a_{M-1})$ and $(b_0, \ldots, b_{M-1})$ are two random vector independent with each other. Besides these, they are also independent of frequency ω. For example, Fig.3.4 shows a simple model with 3 subwindows.

We assume that the measurements are given by:

$$x_m[n] \;=\; s_m[n] + w_m[n] \tag{3.4.3}$$

where $x_m[n]$ is the received signal. $w_m[n]$is a sequence of independent, identically distributed zero mean Gaussian noise with unknown variance σ^2. Assume we start sample at

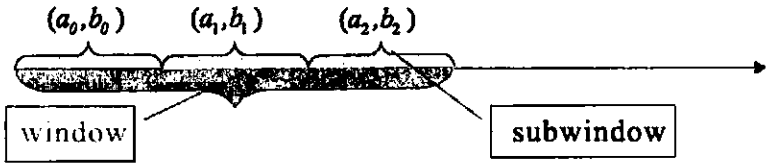

Figure 3.4: Heartbeat Signal Model

$t = 0$. If not, we can combine the initial phase into θ, then

$$s_m[n] = A_m \cos(\omega t_{mn} + \theta_m) = a_m \cos(\omega t_{mn}) + b_m \sin(\omega t_{mn}) \quad (3.4.4)$$

$$t_{mn} = (m \cdot N + n)T \quad (3.4.5)$$

The joint density function for the random sample $\mathbf{x} = (x_0, x_1, \ldots, x_{MN-1})$ is the product density

$$f_{\Theta}(\mathbf{x}; H_1) = (2\pi\sigma^2)^{-MN/2} \exp\{-\frac{1}{2\sigma^2} \sum_{m=0}^{M-1} \sum_{n=0}^{N-1} (x_m[n] - s_m[n])^2\} \quad (3.4.6)$$

$$\Theta = [\omega, \bar{\mathbf{a}}, \bar{\mathbf{b}}, \sigma^2] \quad (3.4.7)$$

Notice that, a_m, b_m and ω are mutual independent.

3.4.2 Heartbeat signal model for complex data

When the record data is complex, the heartbeat signal model is slightly different. In Chapter 1, we know that, the received baseband signal due to heartbeat is given by

$$I \approx -A \sin(\varphi)\omega_c h(t) + Re\{w(t)\} \quad (3.4.8)$$

$$Q \approx A \cos(\varphi)\omega_c h(t) + Im\{w(t)\}$$

$h(t)$ is the heartbeat signal Here ω_c is the RF transmission frequency. φ depends on the DOA and distance between subject and antennas. In the following discussion, the DC offset of data I and Q are all removed.

For each window, assume the mth subwindow, nth sample can be given by:

$$z_m[n] = s_m[n] + w_m[n] = x_m[n] + jy_m[n] \tag{3.4.9}$$

where $(x_m[n], y_m[n])$ is the received I and Q data. $w_m[n]$ is a sequence of independent, identically distributed zero mean complex Gaussian noise with unknown variance σ^2. And assume A_m and B_m are the magnitudes for I and Q:

$$\begin{aligned} A_m &= -A\sin(\varphi)\omega = C\cos(\psi) \\ B_m &= A\cos(\varphi)\omega = C\sin(\psi) \end{aligned} \tag{3.4.10}$$

C is constant, then it can be combined into a_m and b_m. ψ is introduced for simplification, which is also constant within a detection window. Then the IQ data can also be given by

$$\begin{aligned} x_m[n] &= A_m\cos(\omega t_{mn} + \theta_m) + Re\{w_m[n]\} \\ &= \cos(\psi)(a_m\cos(\omega t_{mn}) + b_m\sin(\omega t_{mn})) + Re\{w_m[n]\} \\ y_m[n] &= B_m\cos(\omega t_{mn} + \theta_m) + Im\{w_m[n]\} \\ &= \sin(\psi)(a_m\cos(\omega t_{mn}) + b_m\sin(\omega t_{mn})) + Im\{w_m[n]\} \\ t_{mn} &= (m\cdot N + n)T \end{aligned} \tag{3.4.11}$$

The joint density function for the random sample $\mathbf{z} = (z_0, z_1, \ldots, z_{MN-1})$ is

$$f_{\Theta}(\mathbf{z}; H_1) = (2\pi\sigma^2)^{-MN}\exp\{-\frac{1}{2\sigma^2}\sum_{m=0}^{M-1}\sum_{n=0}^{N-1}\|z_m[n] - s_m[n]\|^2\} \tag{3.4.12}$$

$$\Theta = [\bar{\omega}, \bar{\mathbf{a}}, \bar{\mathbf{b}}, \psi, \sigma^2] \tag{3.4.13}$$

Notice that, a_m, b_m, ω, and ψ are mutual independent.

3.5 Conclusion about heartbeat signal model

In this chapter, a heartbeat signal model is presented, which treats heartbeat signal as a time-varying sinusoid. We divide each detection window into M subwindows with the

same length N. We assume the heartbeat frequency remains constant within each detection window. The magnitude and phase also remain constant within each subwindow, while they jumpily change per subwindow. The noise is WGN with unknown variance. Notice that, We should select reasonable M and N to make let the resulting SNR as high as possible.

Under this model, as to determination of the number of subjects in a given area, the problem reduces to detect the number of single tones with the characteristics described above.

Chapter 4

Detection of Heartbeats

4.1 Methods to detect the number of sinusoids

The problem of jointly detecting the number and estimating the frequencies of multiple sinusoids embedded in noise is a fundamental problem and has received considerable attention in the past several decades. In the first phase of our project, we only aim to detect the number of sinusoids (heartbeats), and this is also a problem of determining the model order.

Several well-known methods have been proposed such as principal components analysis (PCA), which make use of the eigenvalue distribution to determine the model order[25]. The estimator is shown to be able to resolve closely spaced sinusoids at lower signal-to-noise ratios than heuristic tests. However, a practical issue encountered in PCA-based approaches to order estimation is that, it is very difficult to determine the cutoff threshold between the eigenvalues caused by signals and noise, in particular, when a change between two adjacent eigenvalues is not significant.

Other methods for model order selection are based on the information theoretic criteria (AIC)[26] introduced by Akaike (1974)and the minimum description length (MDL)[27] introduced by Schwartz and Rissanen(1978). The number of signals is then

determined as the value for which the criterion is minimized. These methods avoid the problems of derivation of test statistics or selection of thresholds, which are both difficult to determine, particularly when the signal model is complex, time-variant, or not known well. However, they can produce misleading results if they are not carefully used. And they also failed to correctly detect the number of sinusoids when the SNR was low and the number of sinusoids was more than two.

We can see, although there exist a number of methods for model order determination as the above statement, they are not strictly based on classical statistical detection and estimation theory, and thus not optimal.

Since our primary objective is to determine the number of subjects among 2/1/0, we prefer to state the problem as simple as a traditional hypothesis tests. First consider if there are two or more or less than two persons present:

$$\begin{aligned} H_1: &\quad >= 2 \text{ persons exist} \\ H_0: &\quad < 2 \text{ person(0 or 1)person exist} \end{aligned} \tag{4.1.1}$$

If the null hypothesis is accepted, another hypothesis test can be proceeded to decide 1 or 0 person exist:

$$\begin{aligned} H_1: &\quad 1 \text{ person exist} \\ H_0: &\quad 0 \text{ person exist} \end{aligned} \tag{4.1.2}$$

4.2 Neyman-Pearson (NP) test and GLRT

In this section we will discuss how to choose an optimal detector for the particular hypothesis tests described as above.

Since there isn't any prior probabilities $P(H_1), P(H_0)$ about how many subjects exist, Bayesian approach is not in consideration. On the contrary, a Neymann-Pearson(NP)test

is appropriate, which attempts to maximize the detection probability P_D for a given false alarm probability P_{FA}.

To implement the NP test, we first inquire whether the data PDF $p(\mathbf{x}; H_1)$ and $p(\mathbf{x}; H_0)$ are known. With the model we assume, the data are signal with unknown parameters plus AWGN, and the signal doesn't obey the linear model. Under both the null and alternative hypothesis, the noise variance, and coefficients of sinusoids are unknown, the detection is a composite problem and no Uniform Most Powerful (UMP) test exists. For a NP criterion with data model like this, the GLRT, the Wald test, the Rao test, or the locally most powerful (LMP) test should be tried[19].

Generally, we try to get MLEs of these unknown parameters first, then replace the unknown parameters with them. The GLRT, the Wald test, and the Rao test, all require MLE under H_0 or H_1 or both. These three approaches have the same performance, but the later two require Fisher information matrix, which is more complex than likelihood ratio computation. In addition to its simple implementation, we prefer to use GLRT as our detector.

Although there is no optimality associated with the GLRT, in practice, it appears to work quite well. However, if we cannot get MLEs of the unknown parameters, or the MLEs require impractical complexity, then we must proceed to other suboptimal approaches.

4.3 MLE of unknown sinusoids

For the problem of estimation of frequency of sinusoids, Fourier transform is the traditional approach, and its resolution limit is $\frac{1}{NT}$, where T, is the sampling interval and N is the number of processed data. To obtain sufficient resolution, padding is often required. When the required resolution is compatible with the available number of data samples, this method has obvious computational advantage.

Some high resolution algorithms are also available, in which the separation between adjacent frequencies to be estimated can be less than the Fourier resolution limit. They can be based on signal subspace decomposition, and the primary approaches in the field include the MUSIC method proposed by Schmidt, the ESPRIT method by Roy and Kailath, and the Minimum-Norm method by Kumaresan and Tufts[29]. Linear prediction or autoregressive models such as Yule Walker [22], or more complex techniques such as forward-backward linear prediction [23], can also be used.

Most of the high resolution methods have excellent performance and can approach the Cramer-Rao bound under high SNR values and with a moderate amount of data. However, the performance of these approaches decrease rapidly once the SNR falls below a certain threshold value (depending on the method). This is called as SNR threshold effect. In addition, all these algorithms require matrix manipulations and result in heavy computational burden when the matrix size is very large.

When the SNR is very low (for example, below 3dB), the mentioned high resolution algorithms cannot be employed. In this case, we should employ the Maximum Likelihood Estimator(MLE)[29], which is theoretically optimum in terms of mean square error for estimation. For the case of estimation of a single frequency, Rife and Boorstyn have shown in [24] that the MLE can be obtained by means of FFT techniques, and it was shown to be of the form

$$\hat{\omega}_{ML} = \max_{\omega} \|X(\omega)\|^2 \tag{4.3.1}$$

In the case of multiple sinusoids, the maximization of the likelihood function is a highly nonlinear, computationally impractical problem. However, if the frequency separation is large enough, the MLE can still be approximated by the frequencies of the highest peaks of the FFT.

It is also deserved to be pointed out that, all the described high-resolution methods require that the number of frequencies to be estimated is known in advance.

4.4 Detection of heartbeats by GLRT

4.4.1 GLRT with single channel

Consider at first the case of single receiver antenna with only the I-component available with at most 2 subjects in range. We begin from the simplest case $M = 1$, in which only one subwindow exists in each detection window. As argued in the previous section, we model the data received in an interval as a mixture of two periodic signals,

$$x[k] = a_1 \cos(\omega_1 kT) + b_1 \sin(\omega_1 kT) + a_2 \cos(\omega_2 kT) + b_2 \sin(\omega_2 kT) + w[k] \quad (4.4.1)$$

where $w[k]$ is white Gaussian noise (WGN) with power σ^2, and $a_1, a_2, b_1, b_2, \omega_1, \omega_2$, and σ^2 are unknown. The problem of determining if there are two or more or less than two persons present can then be stated as the following hypothesis test problem

$$H_1: \quad (a_1, b_1) \neq (0,0), (a_2, b_2) \neq (0,0) \quad (4.4.2)$$

$$H_0: \quad (a_2, b_2) = (0,0) \quad (4.4.3)$$

This is a composite hypothesis test problem with many unknown parameters, and the best detector for this kind of problem is commonly accepted to be the generalized likelihood ratio test (GLRT) . In the GLRT the following test statistic is defined

$$t(\mathbf{x}) = \frac{\max_{a_1,b_1,a_2,b_2,\omega_1,\omega_2,\sigma^2} f(\mathbf{x})}{\max_{a_1,b_1,a_2=0,b_2=0,\omega_1,\omega_2,\sigma^2} f(\mathbf{x})} \quad (4.4.4)$$

where $f(\mathbf{x})$ is the likelihood function (probability density function) for the received data $\vec{\mathbf{x}} = \{x[0], \ldots, x[N-1]\}$. If $t(\mathbf{x}) > t$, where t is some threshold, the GLRT decides H_1 (two or more persons), otherwise H_0 (less than two persons). The threshold t is determined so that a desired false alarm probability is guaranteed. If H_0 is decided, another GLRT can then be used to decide between 0 and 1 subject.

In the Gaussian case, the GLRT test statistic can be simplified to

$$t(\mathbf{x}) = \frac{\min_{a_1,b_1,\omega_1,} \sum_{k=1}^{N} \{x[k] - a_1 \cos(\omega_1 kT) - b_1 \sin(\omega_1 kT)\}^2}{\min_{a_1,b_1,a_2,b_2,\omega_1,\omega_2} \sum_{k=1}^{N} \{x[k] - \sum_{i=1}^{2} [a_i \cos(\omega_i kT) + b_i \sin(\omega_i kT)]\}^2} \quad (4.4.5)$$

The minimization over (a_1, b_1, a_2, b_2) is a linear problem, but the minimization over (ω_1, ω_2) is a non-linear problem. Although there are effective approaches such as the Prony's and MUSIC methods to find the frequencies. However, these methods can not ensure good performance when be applied to signals with very low SNR as wireless heartbeat signals have. This paper's main focus is not the approach to find these frequencies, so we currently solve this problem just by using a simple grid search to make sure it's optimal as Maximum Likelihood Estimator (MLE).

4.4.2 Extension to multiple channels

Assume that there are multiple receiver antennas with both I and Q-components, and that multipath is negligible. The received signal can then be modeled by

$$\begin{aligned} x[k] = \quad & (a_1 \cos(\omega_1 kT) + b_1 \sin(\omega_1 kT))\mathbf{s}(\phi_1) \\ & +(a_2 \cos(\omega_2 kT) + b_2 \sin(\omega_2 kT))\mathbf{s}(\phi_2) + \mathbf{w}[k] \\ \mathbf{s}(\phi) = \quad & [1, \exp(j\phi), \ldots, \exp(j(M-1)\phi)]^T \end{aligned} \tag{4.4.6}$$

The GLRT test statistic is now

$$t(\mathbf{x}) = \frac{\min \sum_{k=1}^{N} \|x[k] - (a_1 \cos(\omega_1 kT) + b_1 \sin(\omega_1 kT)\mathbf{s}(\phi_1))\|^2}{\min \sum_{k=1}^{N} \|x[k] - \sum_{i=1}^{2}(a_i \cos(\omega_i kT) + b_i \sin(\omega_i kT)\mathbf{s}(\phi_i))\|^2} \tag{4.4.7}$$

Now the minimization $\omega_1, \omega_2, f_1, f_2$ is a non-linear problem solved also by using a simple grid search. Notice that the minimization with respect to f_1, f_2 give DOA as a by-product, so the methods can also be used to localize subjects.

4.5 Data requirement to be successfully detected

After the signal model and detector design are done, another problem comes up: what kind of data we can successfully perform detection? To determine the number of

subjects and locate them, we hope they have different characteristics. Generally, a wireless signal can be depicted in time domain, frequency domain, or spatial domain. In this detection problem, for baseband signal $Ae^{j\varphi}(1 + j\omega x(t))$, only basic phase delay φ contains spatial information, which is determined by distance and DOA between subjects and receiving antennas. In frequency domain, we refer to the heartbeat frequency. In time domain, since all subjects' information mix up together, it's hard to separate them in time domain. We then hope different subjects have different properties in frequency domain or spatial domain, or both. They must be different in at least one domain, otherwise, detection will fail. That's mean, if heartbeats of two person are different enough, no matter in frequency or distance and DOA, we can separate them.

To illustrate the difference, we can turn to IQ constellation, which plots quadrature data versus inphase data. As to the heartbeat frequency, if the heartbeats periodically shift along this line, instead of randomly shifting, that means the heartbeat regularly and heart variation isn't too heavy. The rate of shifting along the line represents the subject's heartbeat frequency, and the slope of the line represents the subject's spatial information (or phase delay) φ.

If two subjects have regular heartbeat with a small or moderate HRV, and their frequency difference is large enough, even though they have the same phase delay φ, we can still separate them. However, heartbeat frequency range is very narrow, only 0.8Hz-2Hz, it's avoidable that some subjects happen to have similar frequencies. Fortunately, due to the carrier's wavelength is very small, different subjects generally have different phase delay φ.

Notice that, only complex data can offer us the information of phase delay φ. If we only use real data, the phase delay φ is combined into the phase of heartbeat, thus we can't estimate it in real data case.

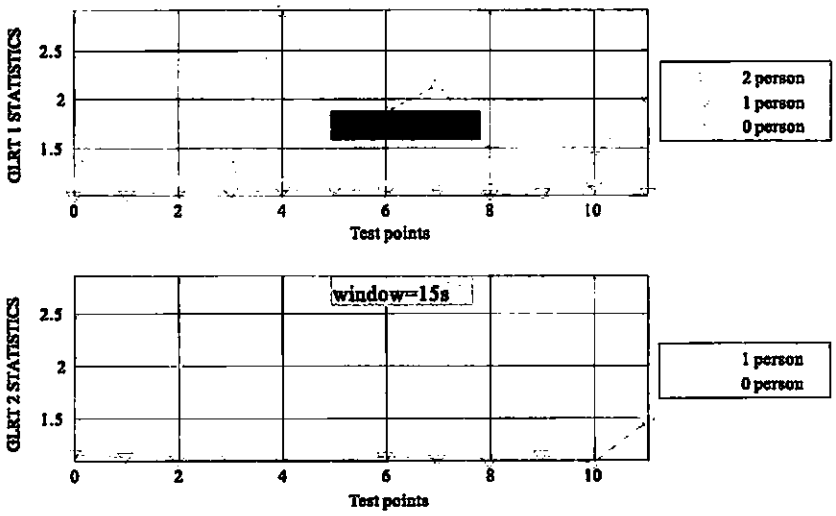

Figure 4.1: Good test result. Top: GLRT, 2 or < 2 subjects. Bottom: GLRT: 1 or 0 subject

4.5.1 GLRT detection results with single channel

We can see the detection result for one window of data. The data are received single channel data, and we assume each detection window only contains one subwindow. Fig.4.1 shows the test statistic applied to a group of three different measurements with single antenna. The measurements are at first filtered with a bandpass filtered with a passband $0.8 \sim 2$Hz to remove respiration and higher order harmonics, and are then divided into (overlapping) intervals of length about 15s. This interval ensures that the model is reasonably accurate, and has been verified through tests with different reference signals. The test statistic is now evaluated in each interval. It shows that it is objectively possible to determine the number of persons, e.g., by using a certain threshold. Notice once it has been determined that less than two persons are present with the above test, another GLRT can then be used to distinguish 0 and 1 persons.

Fig.4.2 shows how the data looks like in time domain. In the top left figure, we can see, the two subjects has different angle, or phase delay φ. When 2 persons are present

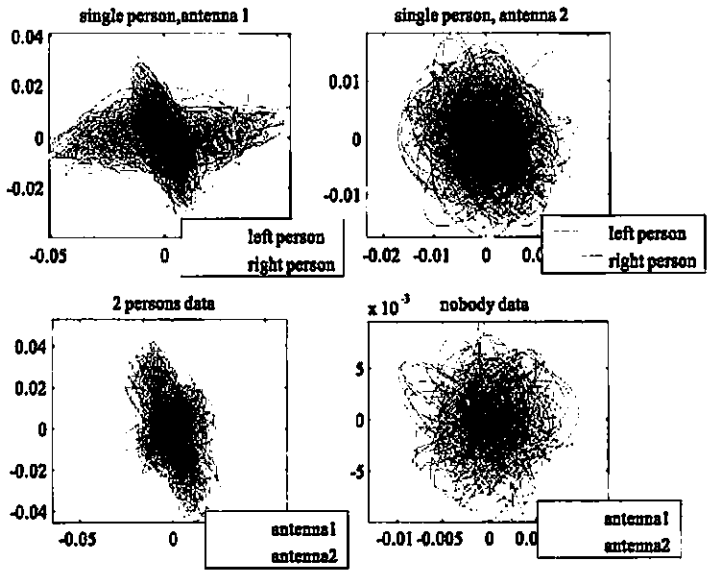

Figure 4.2: IQ constellation of Good test result

at the same time, the data diverge along two different line. The right bottom figure shows that the noise variance is small.

However, results do not always turn out as well as in Fig.4.1. Fig.4.3 shows a figure of bad results. It's hard to apply thresholds to both tests. Fig.4.4 shows how the data looks like in time domain.

We can see, test for subjects with strong HRV is sometimes not detected. And test intervals of length about 15s might not be suitable for effective detection either. To remedy this either the SNR has to be improved, or multiple antennas applied.

We do not yet have a working experimental setup with multiple antennas. Multiple antenna data is therefore obtained from partial simulation. Reference signals are measured for different persons. They are then multiplied with DOA vectors, and independent noise is added at each antenna. Fig.4.5, Fig.4.6, and Fig.4.7 shows some results. In this case we used test subject with strong HRV. With single antenna it is therefore difficult to

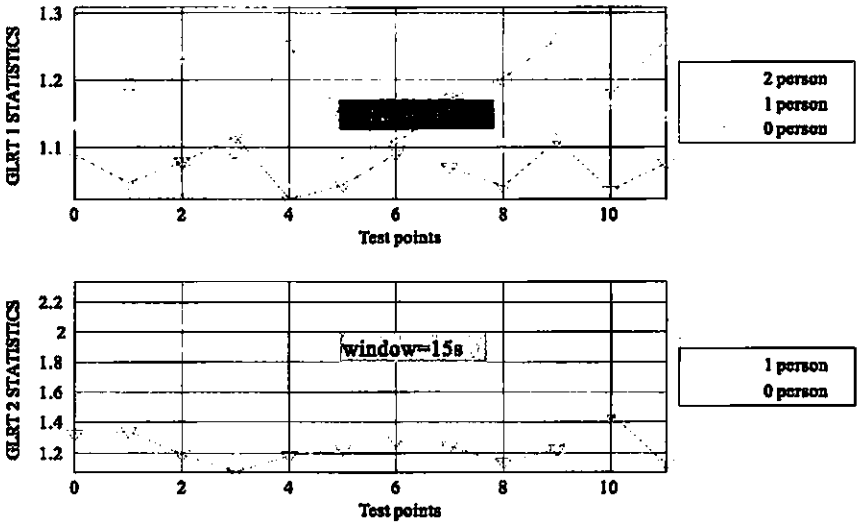

Figure 4.3: Bad test result. Top: GLRT, 2 or < 2 subjects. Bottom: GLRT: 1 or 0 subject

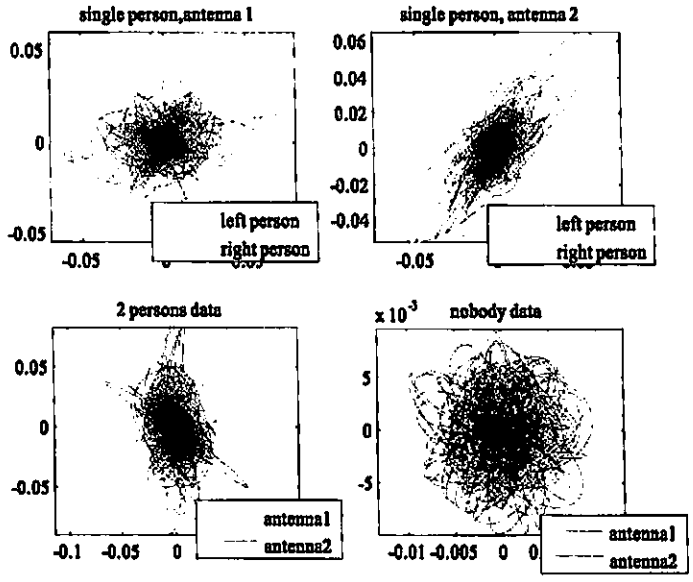

Figure 4.4: IQ constellation of Good test result

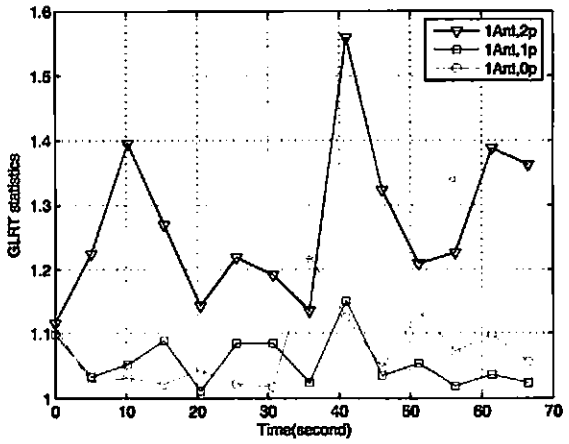

Figure 4.5: Comparison: GLRT for 2/1/0 person with single antenna

detect reliably if there are 1 or 2 subjects. With more antennas, the test statistics tend to fluctuate less. Therefore, it is clearly possible to distinguish these situations by set reasonable thresholds. Although we didn't do nested hypothesis test for 4 antennas, we can see it has the potential to detect up to 2N-1 subjects with N antennas, while MUSIC and other SVD-based approaches can only detect N-1 subjects.

4.5.2 Conclusions about detection

Although we are dealing with very weak and complicated heartbeat signals, we have shown that it is possible to determine the number of subjects within range by using hypothesis testing. For real data model, the method has potential of detecting up to 2N subjects with N antennas. However, for some datasets, the detection performance is not satisfactory. We could possibly get improvement by taking into account more characteristics of the signals, for example, the spatial information embedded in complex data.

On the other hand, the current method is very computationally complex. It can be simplified by using an approximate minimization, for example by using 2D FFT and

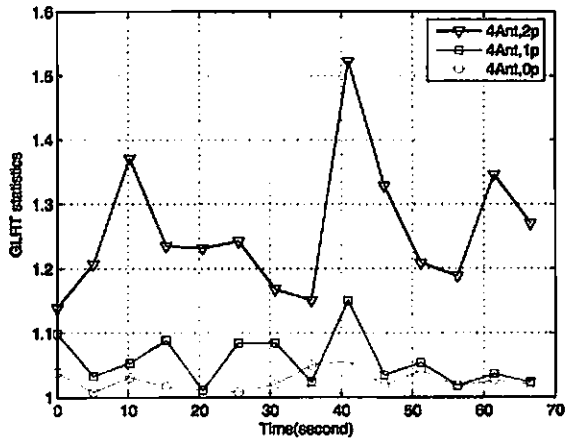

Figure 4.6: Comparison: GLRT for 2/1/0 person with 2 antennas

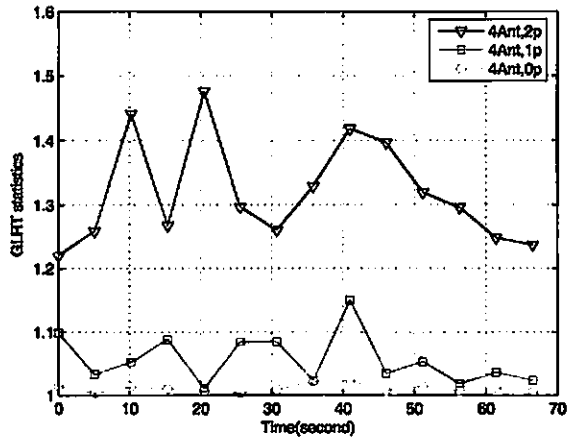

Figure 4.7: Comparison: GLRT for 2/1/0 person with 4 antennas

peak search. If there is heavy multipath the current method cannot be used. Essentially, the method used is a spatio-temporal DOA. With heavy multipath blind source separation methods must be used, for example methods inspired by space-time MUSIC [38][39][40]. Finally, we are also working on extracting heart rate and HRV from the data, but this is beyond the scope of the current paper.

Furthermore, the performance should be evaluated. We did some simulation and it was shown that the performance is highly affected by the test window length. It costs a lot of time to find the best window length. Furthermore, to achieve a effective practical detector, for a given false alarm probability, we must find suitable thresholds that can be applied to test statistics of all measurement. However, the current result is unstable and not satisfactory. In the case of low SNR and large HRV noise, the performance drops significantly. Due to this, the detection probability won't be discussed here.

According to detection theories, the poor performance is attributed to two reasons: poor signal model or unsuitable detection criterion. In this chapter, we only consider single subwindow (M=1).

In terms of signal model, two factors can cause bad performance. Firstly, improper Model can lead too much HRV to be considered as noise by mistake. The resulting SNR would be too low. Secondly, improper window/subwindow length can also contribute to low detection power. The subwindow should be short enough to assure that magnitude, phase and frequency won't change within each subwindow. The window length shouldn't be too long yet, to make sure that heartbeat frequency can be considered as constant during each window. Since heartbeat signal is nonstationary, extra length of data is helpless, or even harmful. Besides these, a window should include enough subwindows to consider heart variation. In a word, it's very important to select the number of subwinodws and reasonable window/subwindow length. We must try to find the best values for these three parameters, therefore to enhance the SNR.

Chapter 5

SVD Combination to Improve the SNR

From Chapter 3, we know that, wireless data's low SNR will cause many detectors invalid. We must try to enhance the SNR. SVD combination is a proposed method. The principle of SVD combination is to decompose the data into 2 orthogonal spaces: signal and noise space. To find these spaces, we need to first evaluate the data's covariance matrix, then use singular value decomposition of this matrix to find these subspaces. We can project the data onto the signal space, the result is the principle components of the data, which maximize the output SNR.

5.1 Difficulties in extracting heartbeat from IQ data

In Chapter 1, the measured I and Q data are given by:

$$\begin{aligned} I &= Re\{Ae^{j\varphi}(1+j\omega x(t))+w(t)\} \\ &\approx A\cos(\varphi)-A\sin(\varphi)\omega x(t)+Re\{w(t)\} \\ Q &= Im\{Ae^{j\varphi}(1+j\omega x(t))+w(t)\} \\ &\approx A\sin(\varphi)-A\cos(\varphi)\omega x(t)+Im\{w(t)\} \end{aligned} \tag{5.1.1}$$

in which φ is unknown and determined by the distance and DOA between the subject and the antenna. There are several difficulties deserve notice:

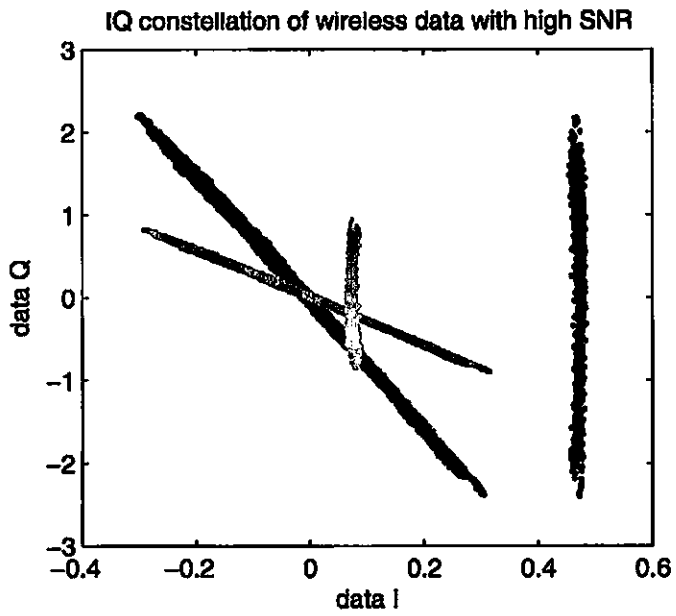

Figure 5.1: The IQ constellation for received data with high SNR

DC component and IQ imbalance We can see, I and Q are complex functions of $x(t)$ and A, φ, ω. I and Q also contain other DC components due to reflections and so on. For simplicity, we remove all DC. Besides DC problem, IQ imbalance is another annoying problem due to our current incomplete antenna design. Therefore, we can not directly use "I + jQ" to denote the complex data. Instead, we need to do some correction.

Enhance of SNR The detection performance is highly related with received signal's SNR. Sometimes the subject's HRV is very heavy and results very low SNR, thus makes detection almost impossible. If we observe the IQ constellation we'll find heartbeat signal no longer changes periodically along a line like in Fig.5.1, on the contrary, it diverges like a cloud as Fig.5.2 shows.

Heartbeat cancelation Although only $x(t)$ contains heartbeat information, since we don't know the position information of subjects beforehand, it's not easy to extract $x(t)$

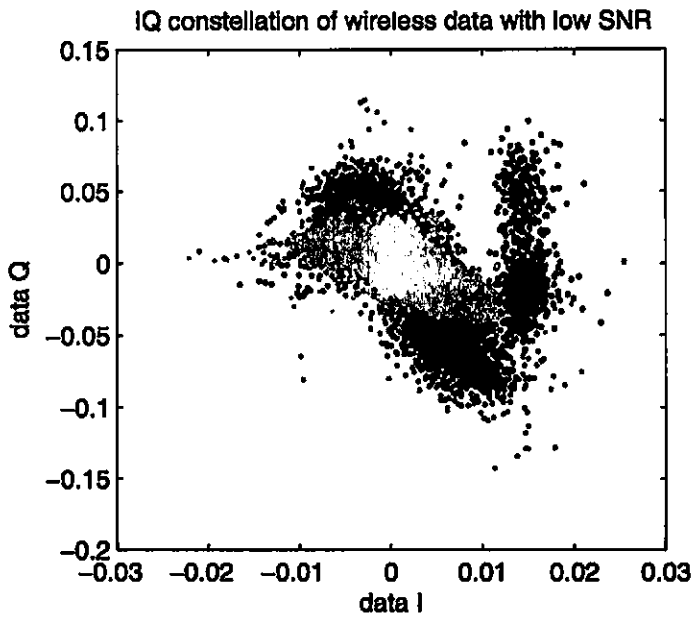

Figure 5.2: The IQ constellation for received data with low SNR

from the IQ data. Furthermore, different position cause different magnitude for $x(t)$ in IQ data. The most unfavorable case is that, when $\varphi = n\pi$, the $x(t)$ in data Q will be canceled since $\cos(\varphi) = 0$. When $\varphi = n\pi/2$, the $x(t)$ in data I will also be canceled. During measurement, φ is a random variable and is beyond the control of testers, hence, we cannot avoid the worst cancelation to happen.

SVD combination in multiple antennas system For all the above problems, MIMO architecture could help out. For multiple antenna system, we can use the idea of maximum ratio combining to get a maximum SNR output. We observe that, both I and Q contains $x(t)$, and they won't be canceled at the same time. After removing the DC offset in data I and Q separately, we can use a SVD combination to find the key random variable $x(t)$. This method will provide the maximum SNR output.

5.2 Introduction to Singular Value Decomposition (SVD)

Some efficient approaches for noise reduction are based on singular value decomposition (SVD). The main idea is to decompose the signal into two time-orthogonal subspaces; one containing the signal and the other containing noise. Actually the unknown key random signals could be considered as an optimal linear combination of subspaces. Since the signal subspace is orthogonal to noise subspace, if we project the received signal into the signal subspace, for the resulting signal, the contamination of noise is removed, thus leading to a less MSE and SNR penalty. It could enhance SNR without any prior information. The critical problem is to find the exact orthogonal subspaces for a particular data record. If the data can be modeled as signal plus white Gaussian noise, SVD is shown to be the MLE of subspaces [29].

Suppose we take a sequence of measurements of the form $\{\mathbf{x}_t\}^{M-1}$. Each measurement is an $N \times 1$ vector of the form

$$\mathbf{x}_t = \mathbf{s}_t + \mathbf{n}_t \tag{5.2.1}$$

The signal vector $\mathbf{s}_t$ is unknown, but they are known to lie in a $p-$dimensional subspace, meaning $\mathbf{s}_t = \mathbf{H}\theta_t$. And there exist $N - p$ linearly independent vectors $\mathbf{a}_i$ such that

$$\mathbf{a}_i^T \mathbf{s}_t = 0, \quad i = p+1, \ldots, N, \quad t = 0, 1, \ldots, M-1. \tag{5.2.2}$$

Assume the observation noises $\{\mathbf{x}_t\}^{M-1}$ are independent and with a distribution $N[\mathbf{0}, \sigma^2\mathbf{I}]$. Then the log-likelihood function for $\{\mathbf{x}_t\}^{M-1}$ is (ignoring constants)

$$L = -\frac{1}{2\sigma^2} \sum_{t=0}^{M-1} (\mathbf{x}_t - \mathbf{s}_t)^T (\mathbf{x}_t - \mathbf{s}_t) \tag{5.2.3}$$

5.3 Maximum likelihood identification of a signal subspace by SVD

We want to find the maximum likelihood the signal subspace H, or equivalently, the orthogonal subspace $\mathbf{A} = [\mathbf{a}_{p+1}, \ldots, \mathbf{a}_N]$. A maximum likelihood principle for identifying the orthogonal subspace $\mathbf{A}$ will maximize log likelihood under the constraints

$$\mathbf{a}_i^T \mathbf{s}_t = 0, \quad i = p+1, \ldots, N, \quad t = 0, 1, \ldots, M-1. \tag{5.3.1}$$

Then form a Lagrangian for minimizing $-2\sigma^2 L$ under these constraints:

$$\xi = \sum_{t=0}^{M-1} (\mathbf{x}_t - \mathbf{s}_t)^T (\mathbf{x}_t - \mathbf{s}_t) + 2 \sum_{i=p+1}^{N} \sum_{t=0}^{M-1} \lambda_{ti} \mathbf{a}_i^T \mathbf{s}_t \tag{5.3.2}$$

Assume the $\mathbf{A}$ is known for the moment, then the candidate solution for $\mathbf{s}_t$ is

$$\begin{aligned} \mathbf{s}_t &= \mathbf{x}_t - \sum_{i=p+1}^{N} \lambda_{ti} \mathbf{a}_i = \mathbf{x}_t - \mathbf{A}\lambda_t \\ \mathbf{A} &= [\mathbf{a}_{p+1}, \ldots, \mathbf{a}_N] \\ \lambda_t &= [\lambda_{t(p+1)}, \ldots, \lambda_{t(N)}] \end{aligned} \tag{5.3.3}$$

The constraints are enforced by writing

$$\mathbf{A}^T (\mathbf{x}_t - \mathbf{A}\lambda_t) = 0 \tag{5.3.4}$$

And solving for λ_t

$$\lambda_t = (\mathbf{A}^T \mathbf{A})^{-1} \mathbf{A}^T \mathbf{x}_t \tag{5.3.5}$$

The corresponding solution for $\mathbf{s}_t$ is

$$\mathbf{s}_t = (\mathbf{I} - (\mathbf{A}^T \mathbf{A})^{-1} \mathbf{A}^T) \mathbf{x}_t = (\mathbf{I} - \mathbf{P}_A) \mathbf{x}_t \tag{5.3.6}$$

The resulting maximum likelihood is

$$L = -\frac{1}{2\sigma^2} \sum_{t=0}^{M-1} \mathbf{x}_t^T \mathbf{P}_A \mathbf{P}_A = -\frac{m}{2\sigma^2} tr[\mathbf{P}_A \mathbf{S}] \tag{5.3.7}$$

$$\mathbf{S} = \frac{1}{M} \sum_{t=0}^{M-1} \mathbf{x}\mathbf{x}_t^T \tag{5.3.8}$$

If $\mathbf{A}$ is unknown, we can get it by *Singular Value Decomposition (SVD)*

$$\begin{aligned} \mathbf{S} &= \mathbf{U}\mathbf{\Lambda}^2\mathbf{U}^T \\ \mathbf{U} &= [\mathbf{u}_1 \dots \mathbf{u}_{p+1} \dots \mathbf{u}_N] \\ \mathbf{\Lambda}^2 &= diag[\lambda_1^2 \dots \lambda_{p+1}^2 \dots \lambda_N^2]; \quad \lambda_1^2 \geq \lambda_2^2 \geq \dots \geq \lambda_N^2 \end{aligned} \tag{5.3.9}$$

And L is bounded as follows:

$$L = -\frac{1}{2\sigma^2}\sum_{t=0}^{M-1}\mathbf{x}_t^T\mathbf{P}_A\mathbf{P}_A = -\frac{m}{2\sigma^2}tr[\mathbf{P}_A\mathbf{S}] \leq -\frac{1}{2\sigma^2}\sum_{i=p+1}^{N}\lambda_i^2 \tag{5.3.10}$$

The bound is achieved for a projector $\mathbf{P}_A$ onto the subspace $\langle \mathbf{U}_{p+1} \rangle$:

$$\begin{aligned} \mathbf{P}_A &= \mathbf{U}_{p+1}\mathbf{U}_{p+1}^T = \sum_{i=p+1}^{N}\mathbf{u}_i\mathbf{u}_i^T \\ \mathbf{U}_{p+1} &= [\mathbf{u}_{p+1} \dots \mathbf{u}_N] \end{aligned} \tag{5.3.11}$$

In summary, maximum likelihood theory builds a rank p subspaces $\langle \mathbf{H} \rangle$ from the dominant p eigenvectors of the sample covariance matrix.

$$\begin{aligned} \mathbf{S} &= \mathbf{U}\mathbf{\Lambda}^2\mathbf{U}^T \\ \mathbf{U} &= [\mathbf{u}_1 \dots \mathbf{u}_{p+1} \dots \mathbf{u}_N] \\ \mathbf{\Lambda}^2 &= diag[\lambda_1^2 \dots \lambda_{p+1}^2 \dots \lambda_N^2]; \quad \lambda_1^2 \geq \lambda_2^2 \geq \dots \geq \lambda_N^2 \\ \hat{\mathbf{P}}_A &= \sum_{i=p+1}^{N}\mathbf{u}_i\mathbf{u}_i^T \\ \hat{\mathbf{H}} &= \mathbf{I} - \hat{\mathbf{P}}_A \\ \hat{\mathbf{s}}_t &= \hat{\mathbf{H}}\mathbf{x}_t = (\mathbf{I} - \hat{\mathbf{P}}_A)\mathbf{x}_t \end{aligned} \tag{5.3.12}$$

$\hat{\mathbf{P}}_A\mathbf{S}\hat{\mathbf{P}}_A$ is the estimated noise covariance matrix and $\hat{\mathbf{H}}\mathbf{S}\hat{\mathbf{H}}$ is the estimated signal covariance matrix.

5.4 Enhance SNR with SVD-combination

When more than one channel data are available, through SVD combination we can improve SNR of the wireless heartbeat signal. In this case, each channel (I or Q)

can be treated as one measurement of heartbeat, and these measurements are real rather than complex. If there are $2N$ channels and each channel recorded L samples, then all the received data can be formulated into an $L \times 2N$ size matrix. No matter how many subjects exist, each channel data is a linear combination of their heartbeats. With the principle component theory, we can find the most significant component of the subjects heartbeat signals by SVD-combination, if only the number of channels would be larger than the number of subjects. We call the resulting signal as a SVD combination signal.

For single and N antennas cases, the received data are separately given by:

$$\begin{aligned} \mathbf{X} &= [\mathbf{I}_{Ant1} \quad \mathbf{Q}_{Ant1}] \quad or \\ \mathbf{X} &= [\mathbf{I}_{Ant1} \quad \mathbf{Q}_{Ant1} \ldots \mathbf{I}_{AntN} \quad \mathbf{Q}_{AntN}] \end{aligned} \tag{5.4.1}$$

For single person case, the most significant component is the projection of data onto the projection vector $\mathbf{U_1}$, which is the eigenvector corresponding the largest eigenvalue. The process to find the most significant component is illustrated as,

$$\begin{aligned} \mathbf{Y} = &\quad cov(\mathbf{X}, \mathbf{X}) \\ [\mathbf{U}, \mathbf{S}, \mathbf{V}] = &\quad svd(\mathbf{Y}) \\ \mathbf{Z} = &\quad \mathbf{X}\mathbf{U_1} \end{aligned} \tag{5.4.2}$$

where Z is the SVD combined signal, and use this signal to do GLRT.

We can observe how SVD combination improve signals in frequency domain and time domain. We got wireless data by 2 antennas (4 channels). In Fig.5.3, due to position or heart variation problem, only one channel, the right top one shows a clear PSD peak matched with that of reference. After SVD combination, the resulting data show clearer heartbeat frequency peak in Fig.5.4. Fig.5.5 compares SVD combination effect in time domain. Before SVD combination, compared with reference signal, most channels show different number of wave peaks within the window. That's mean, they have different main

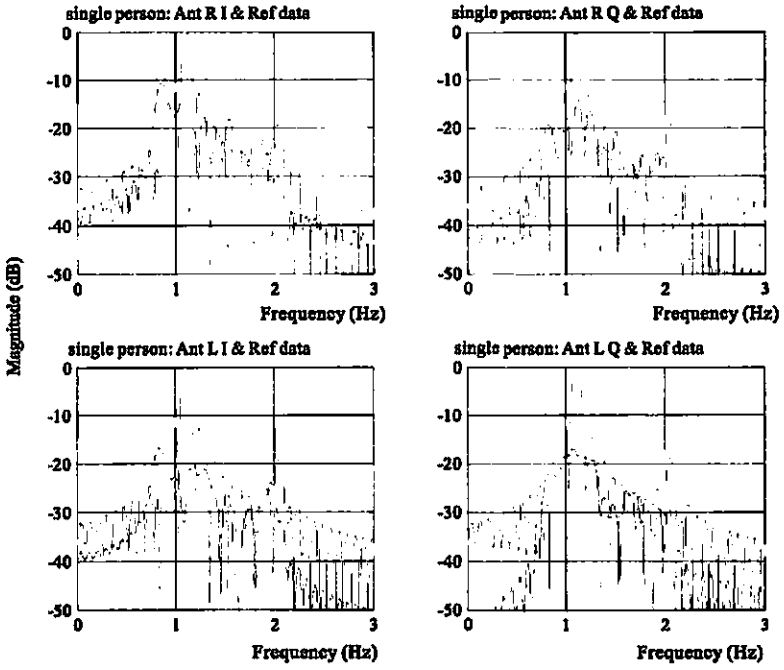

Figure 5.3: Comparison: PSD of 4 channels data

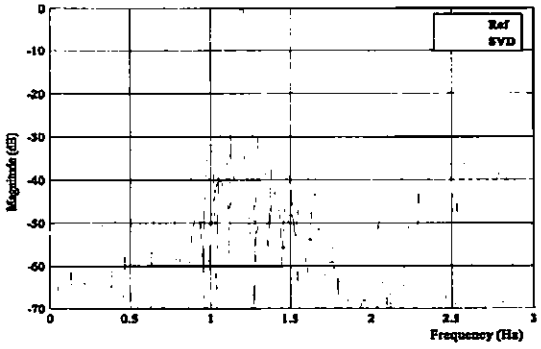

Figure 5.4: Comparison: PSD of SVD-combined data

frequency in comparison with reference signal. After SVD combination, the resulting data agrees with the reference data more smoothly.

SVD combination scheme can maximize the output SNR, therefore, it can obtain higher detection performance compared with single channel. However, if the projection matrix is not accurate, SVD combination's effect will be attenuated. On the other hand, in MIMO system with plentiful multipath, more channels can improve signal's SNR better. Thus, in heartbeat detection, more channels are also helpful to improve the detection performance.

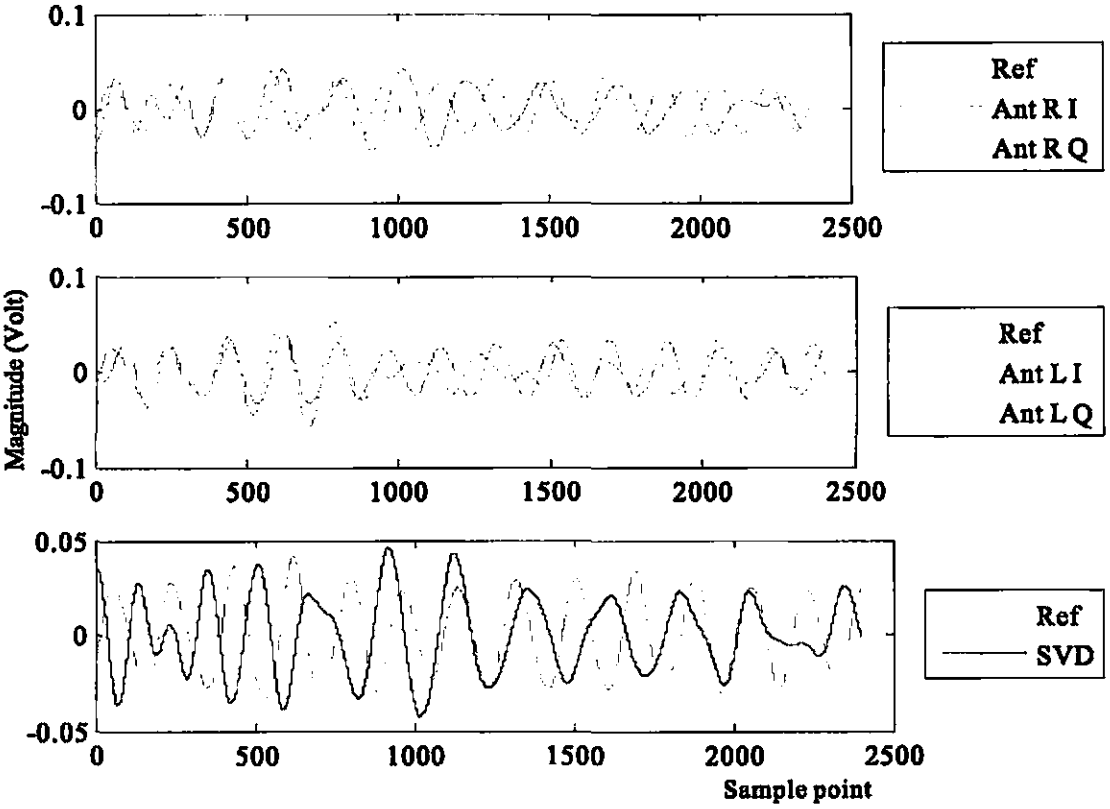

Figure 5.5: Comparison: SVD-combined data and complex data in time domain

Chapter 6

Fast FFT-GLRT-based Detection

Since the heartbeat signal embedded in inphase and quadrature phase data in different ways, we can use real signal (I or Q) or complex signal to perform detection, the resulting detectors are slightly different. In this chapter, detectors for real and complex model are derived, which are both based on GLRT. These two detectors and their performance analysis are compared. For real model, we can use SVD Combination to combine all channels data to extract heartbeat signal. The resulting signal is the principle component of heartbeat signal, with maximal output SNR among all I and Q channels.

For GLRT, we need to solve MLE of unknown parameters first. However, when multiple subjects exist, this is a very difficult problem. In the following discussion, for simplicity and time reason, we only consider the detection problem about whether single person or nobody exists. As a result, the detector is based on FFT and GLRT, which can be easily and simply implemented. Thus, we call them **FFT-GLRT-based Detectors.**

6.1 Detection for real data model

6.1.1 GLRT and MLE of parameters when noise is unknown

Assume the data received is real. We perform detection frame by frame with length of MN. Each frame can be divided into M subwindows, which contains N samples.

We assume that the measurements are given by:

$$x_m[n] = s_m[n] + w_m[n] \tag{6.1.1}$$

where $x_m[n]$ is the received signal. $w_m[n]$is a sequence of independent, identically distributed zero mean Gaussian noise with unknown variance σ^2. Assume we start sample at $t = 0$. If not, we can combine the initial phase into θ_m, then

$$s_m[n] = A_m \cos(\omega t_{mn} + \theta_m) = a_m \cos(\omega t_{mn}) + b_m \sin(\omega t_{mn}) \tag{6.1.2}$$

$$t_{mn} = (m \cdot N + n)T \tag{6.1.3}$$

The joint density function for the random sample $\mathbf{x} = (x_0, x_1, \ldots, x_{MN-1})$ is the product density

$$f_{\Theta}(\mathbf{x}; H_1) = (2\pi\sigma^2)^{-MN/2} \exp\{-\frac{1}{2\sigma^2} \sum_{m=0}^{M-1} \sum_{n=0}^{N-1} [(x_m[n] - s_m[n])^2]\} \tag{6.1.4}$$

$$\Theta = [\omega, \bar{\mathbf{a}}, \bar{\mathbf{b}}, \sigma^2] \tag{6.1.5}$$

The first thing is to find the maximum likelihood estimate of Θ, especially the frequency ω. Let's maximize the log-likelihood $L_{\Theta}(\mathbf{x}; H_1) = \ln f_{\Theta}(\mathbf{x})$ first with respect ro σ^2:

$$\frac{\partial}{\partial\sigma^2} L_{\Theta}(\mathbf{x}; H_1) = -\frac{MN}{2\sigma^2} + \frac{1}{2\sigma^4} \sum_{m=0}^{M-1} \sum_{n=0}^{N-1} (x_m[n] - s_m[n])^2 = 0 \tag{6.1.6}$$

Define the square error γ^2 and γ_m^2 as

$$\gamma_m^2 = \sum_{n=0}^{N-1} (x_m[n] - s_m[n])^2 \tag{6.1.7}$$

$$\gamma^2 = \sum_{m=0}^{M-1} \sum_{n=0}^{N-1} (x_m[n] - s_m[n])^2 = \sum_{m=0}^{M-1} \gamma_m^2 \tag{6.1.8}$$

So the maximum likelihood estimate of $\sigma^2$is

$$\hat{\sigma^2} = \frac{1}{MN}\gamma^2 = \frac{1}{MN} \sum_{m=0}^{M-1} \sum_{n=0}^{N-1} (x_m[n] - s_m[n])^2 \tag{6.1.9}$$

Thus, we have the likelihood and log-likelihood as

$$\begin{aligned} f_{\Theta}(\mathbf{x}; H_1) &= (2\pi\hat{\sigma^2})^{-\frac{MN}{2}} \exp\{-\frac{MN}{2}\} \\ L_{\Theta}(\mathbf{x}; H_1) &= -\frac{MN}{2}\ln(2\pi\hat{\sigma^2}) - \frac{MN}{2} \end{aligned} \tag{6.1.10}$$

To maximize the log-likelihood $L_{\Theta}(\mathbf{x}; H_1)$ is equivalent to minimize the square error γ^2, the summation of γ_m^2 over$m$. Since γ_m^2. Each item of γ_m^2 contain unknown parameters ω, a_m, b_m. To determine them, we firstly expand γ_m^2 with them:

$$\begin{aligned} \sum_{n=0}^{N-1}[(x_m[n] - s_m[n])^2] &= \sum_{n=0}^{N-1}[x_m[n] - a_m\cos(\omega t_{mn}) - b_m\sin(\omega t_{mn})]^2 \\ &= \sum_{n=0}^{N-1} x_m[n]^2 + a_m b_m \sum_{n=0}^{N-1}\sin(2\omega t_{mn}) \\ &+ a_m^2\sum_{n=0}^{N-1}\cos^2(\omega t_{mn}) + b_m^2\sum_{n=0}^{N-1}\sin^2(\omega t_{mn}) \\ &- a_m[\sum_{n=0}^{N-1} x_m[n](e^{-jn\omega T}e^{-jmN\omega T} + e^{jn\omega T}e^{jmN\omega T})] \\ &+ jb_m[\sum_{n=0}^{N-1} x_m[n](e^{-jn\omega T}e^{-jmN\omega T} - e^{jn\omega T}e^{jmN\omega T})] \end{aligned} \tag{6.1.11}$$

From the definition of Discrete Fourier Transform(DFT),

$$X_m(\omega) = \sum_{n=0}^{N-1} x_m[n]e^{-jn\omega T} \tag{6.1.12}$$

in connection with approximation

$$\begin{aligned} \sum_{n=0}^{N-1}\cos(\omega t_{mn})^2 &\approx \frac{N}{2} \\ \sum_{n=0}^{N-1}\sin(\omega t_{mn})^2 &\approx \frac{N}{2} \\ \sum_{n=0}^{N-1}\sin(2\omega t_{mn}) &\approx 0 \end{aligned} \tag{6.1.13}$$

we can derive

$$\begin{aligned} \gamma_m^2 &= \sum_{n=0}^{N-1} x_m[n]^2 + \frac{N}{2}(a_m^2 + b_m^2) \\ &- a_m[X_m(\omega)e^{-jmN\omega T} + X_m(-\omega)e^{jmN\omega T}] \\ &+ jb_m[X_m(\omega)e^{-jmN\omega T} - X_m(-\omega)e^{jmN\omega T}] \end{aligned} \tag{6.1.14}$$

Because x_m is real,

$$X_m(-\omega)e^{jmN\omega T} = \{X_m(\omega)e^{-jmN\omega T}\}^* \tag{6.1.15}$$

Then

$$\begin{aligned}\gamma_m^2 &= \sum_{n=0}^{N-1} x_m[n]^2 + \frac{N}{2}(a_m^2 + b_m^2) \\ &- 2a_m Re[X_m(\omega)e^{-jmN\omega T}] + 2b_m Im[X_m(\omega)e^{-jmN\omega T}]\end{aligned} \tag{6.1.16}$$

As we assumed, phase jumps and magnitude changes from subwindow to subwindow, then the parameters a_m, b_m are independent with each other. Take first derivative to get solutions of a_m, b_m that make the square error γ^2 minimal,

$$\frac{\partial \gamma^2}{\partial a_m} = \frac{\partial \gamma_m^2}{\partial a_m} = Na_m - 2Re[X_m(\omega)e^{-jmN\omega T}] \tag{6.1.17}$$

By taking derivative with b_m too, we get the solutions:

$$\hat{a}_m = \frac{2}{N} Re[X_m(\omega)e^{-jmN\omega T}] \tag{6.1.18}$$

$$\hat{b}_m = -\frac{2}{N} Im[X_m(\omega)e^{-jmN\omega T}] \tag{6.1.19}$$

And γ_m^2 can be given as

$$\begin{aligned}\gamma_m^2 &= \sum_{n=0}^{N-1} x_m^2[n] - \frac{N}{2}(\hat{a}_m^2 + \hat{b}_m^2) \\ &= \sum_{n=0}^{N-1} x_m^2[n] - \frac{2}{N}\|X_m(\omega)e^{-jmN\omega T}\|^2 \\ &= \sum_{n=0}^{N-1} x_m^2[n] - \frac{2}{N}\|X_m(\omega)\|^2\end{aligned} \tag{6.1.20}$$

Hence, to maximize the log-likelihood $L_{\Theta}(\mathbf{x}; H_1)$ is equivalent to minimizing

$$\gamma^2 = \sum_{m=0}^{M-1}\sum_{n=0}^{N-1} x_m^2[n] - \frac{2}{N}\sum_{m=0}^{M-1}\|X_m(\omega)\|^2 \tag{6.1.21}$$

For fixed M and N, the value of γ^2 only depends on ω now, thus the maximum likelihood estimate of ω :

$$\hat{\omega}_{ML} = \max_{\omega} \frac{1}{M}\sum_{m=0}^{M-1}\|X_m(\omega)\|^2 \tag{6.1.22}$$

Finally, we summarize all the parameter estimations under H_1 hypothesis:

$$\begin{aligned}
\hat{\omega}_{ML} &= \max_{\omega} \frac{1}{M} \sum_{m=0}^{M-1} \|X_m(\omega)\|^2 \\
\hat{a}_m &= \frac{2}{N} Re\{X_m(\hat{\omega}) e^{-jmN\hat{\omega}T}\} \\
\hat{b}_m &= -\frac{2}{N} Im\{X_m(\hat{\omega}) e^{-jmN\hat{\omega}T}\} \\
\hat{\sigma_1^2} &= \frac{1}{MN}\{\sum_{m=0}^{M-1}\sum_{n=0}^{N-1} x_m^2[n] - \frac{2}{N}\sum_{m=0}^{M-1}\|X_m(\hat{\omega})\|^2\} \\
f_{\Theta}(\mathbf{x}; H_1) &= (2\pi\hat{\sigma_1^2})^{-\frac{MN}{2}} \exp(-\frac{MN}{2})
\end{aligned} \tag{6.1.23}$$

Under H_0 hypothesis,we only need to estimate the noise variance:

$$\begin{aligned}
\hat{\sigma_0^2} &= \frac{1}{MN}\sum_{m=0}^{M-1}\sum_{n=0}^{N-1} x_m^2[n] \\
f_{\Theta}(\mathbf{x}; H_0) &= (2\pi\hat{\sigma_0^2})^{-\frac{MN}{2}} \exp(-\frac{MN}{2})
\end{aligned} \tag{6.1.24}$$

Now we can represent the likelihood ratio for hypothesis H_1 and H_0 as

$$L_{\mathbf{G}}(\mathbf{x}) = \frac{f_{\Theta}(\mathbf{x}; H_1)}{f_{\Theta}(\mathbf{x}; H_0)} = (\frac{\hat{\sigma_1^2}}{\hat{\sigma_0^2}})^{-\frac{MN}{2}} \tag{6.1.25}$$

Since M and N are known, the test statistics is expressed as

$$\begin{aligned}
t_{\mathbf{G}}(\mathbf{x}) &= \frac{\sum_{m=0}^{M-1}\sum_{n=0}^{N-1} x_m^2[n]}{\sum_{m=0}^{M-1}\sum_{n=0}^{N-1}[x_m[n] - \hat{a}_m\cos(\hat{\omega}t_{mn}) - \hat{b}_m\sin(\hat{\omega}t_{mn})]^2} \\
&= \frac{\sum_{m=0}^{M-1}\sum_{n=0}^{N-1} x_m^2[n]}{\sum_{m=0}^{M-1}\sum_{n=0}^{N-1} x_m^2[n] - \frac{2}{N}\sum_{m=0}^{M-1}\|X_m(\hat{\omega}_{ML})\|^2}
\end{aligned} \tag{6.1.26}$$

To get test statistics, we only need to evaluate the power of received signal, and search the peak of averaged PSD. Since we only interested in the narrow range of heartbeat frequency (0.8~2Hz), to speed the processing, we can use Goertzel algorithm instead of classical FFT.

6.1.2 GLRT and MLE of parameters when noise is known

In the case of known noise, the joint density function for the random process of $x(\Theta, t)$ is almost the same, and the only difference is that the random vector Θ doesn't

include σ^2 any more

$$
\begin{aligned}
f_{\Theta}(\mathbf{x}; H_1) &= (2\pi\sigma^2)^{-MN/2} \exp\{-\frac{1}{2\sigma^2} \sum_{m=0}^{M-1} \sum_{n=0}^{N-1} [(x_m[n] - s_m[n])^2]\} \quad (6.1.27) \\
f_{\Theta}(\mathbf{x}; H_0) &= (2\pi\sigma^2)^{-MN/2} \exp\{-\frac{1}{2\sigma^2} \sum_{m=0}^{M-1} \sum_{n=0}^{N-1} x_m^2[n]\} \\
\Theta &= [\omega, \bar{\mathbf{a}}, \bar{\mathbf{b}}]
\end{aligned}
$$

The likelihood ratio for hypothesis H_1 and H_0 can be denoted as

$$
L_G(\mathbf{x}) = \frac{\exp\{\frac{1}{2\sigma^2} \sum_{m=0}^{M-1} \sum_{n=0}^{N-1} x_m^2[n]\}}{\exp\{\frac{1}{2\sigma^2} \sum_{m=0}^{M-1} \sum_{n=0}^{N-1} [x_m[n] - \hat{a}_m \cos(\hat{\omega} t_{mn}) - \hat{b}_m \sin(\hat{\omega} t_{mn})]^2\}} \quad (6.1.28)
$$

When M and N are known, after taking logarithm of the likelihood ratio,the test statistics is expressed as

$$
\begin{aligned}
t_G(\mathbf{x}) = & \frac{1}{2\sigma^2}\{\sum_{m=0}^{M-1} \sum_{n=0}^{N-1} x_m^2[n] \quad (6.1.29) \\
& - \sum_{m=0}^{M-1} \sum_{n=0}^{N-1} [x_m[n] - \hat{a}_m \cos(\hat{\omega} t_{mn}) - \hat{b}_m \sin(\hat{\omega} t_{mn})]^2\} \\
= & \frac{1}{2\sigma^2}\{\sum_{m=0}^{M-1} \sum_{n=0}^{N-1} x_m^2[n] - (\sum_{m=0}^{M-1} \sum_{n=0}^{N-1} x_m^2[n] - \frac{2}{N} \sum_{m=0}^{M-1} \|X_m(\hat{\omega})\|^2)\} \\
= & \frac{1}{N\sigma^2} \sum_{m=0}^{M-1} \|X_m(\hat{\omega}_{ML})\|^2
\end{aligned}
$$

6.2 Detection for complex data model

In SVD combination, we didn't exploit the characteristics of DOA and distance of each subject. However, these characteristics are beneficial to identify subjects, especially when multiple subjects present. Although the SVD combined data can provide a higher accuracy for frequency estimation, it doesn't assure to result a better detection performance. If the IQ measurement is correct, the complex data should perform better in detection, because it contains more information than SVD combined data. We will investigate how to use data of both IQ channels more efficiently, and evaluate its detection performance.

For each window, assume the mth subwindow, nth sample can be given by:

$$z_m[n] = s_m[n] + w_m[n] = x_m[n] + jy_m[n] \tag{6.2.1}$$

where $(x_m[n], y_m[n])$ is the received I and Q data; $w_m[n]$ is a sequence of independent, identically distributed zero mean complex Gaussian noise with unknown variance σ^2. Assume A_m and B_m are the magnitudes for I and Q:

$$\begin{aligned} A_m &= -A\sin(\varphi)\omega_c = C\cos(\psi) \\ B_m &= A\cos(\varphi)\omega_c = C\sin(\psi) \end{aligned} \tag{6.2.2}$$

C is constant, then it can be combined into a_m and b_m. ψ is introduced for simplification, which is also constant within a detection window. Then the IQ data can also be given by

$$\begin{aligned} x_m[n] &= A_m\cos(\omega t_{mn} + \theta_m) + Re\{w_m[n]\} \\ &= \cos(\psi)[a_m\cos(\omega t_{mn}) + b_m\sin(\omega t_{mn})] + Re\{w_m[n]\} \\ y_m[n] &= B_m\cos(\omega t_{mn} + \theta_m) + Im\{w_m[n]\} \\ &= \sin(\psi)[a_m\cos(\omega t_{mn}) + b_m\sin(\omega t_{mn})] + Im\{w_m[n]\} \\ t_{mn} &= (m\cdot N + n)T \end{aligned} \tag{6.2.3}$$

The joint density function for the random sample $\mathbf{z} = (z_0, z_1, \ldots, z_{MN-1})$ is

$$f_\Theta(\mathbf{z}; H_1) = (2\pi\sigma^2)^{-MN}\exp\{-\frac{1}{2\sigma^2}\sum_{m=0}^{M-1}\sum_{n=0}^{N-1}\|z_m[n] - s_m[n]\|^2\} \tag{6.2.4}$$

$$\Theta = [\omega, \bar{\mathbf{a}}, \bar{\mathbf{b}}, \psi, \sigma^2] \tag{6.2.5}$$

The magnitude and DOA are independent of the heartbeat's frequency and phase. Hence, ψ is independent of ω, a_m, b_m. The square error $\gamma^2 = \sum_{m=0}^{M-1}\gamma_m^2$ and γ_m^2 can by represented as

$$\gamma_m^2 = \sum_{n=0}^{N-1} x_m[n]^2 + \sum_{n=0}^{N-1} y_m[n]^2 \tag{6.2.6}$$

$$
\begin{aligned}
+ \quad & \{a_m b_m \sum_{n=0}^{N-1} \sin(2\omega t_{mn}) + a_m^2 \sum_{n=0}^{N-1} \cos^2(\omega t_{mn}) + b_m^2 \sum_{n=0}^{N-1} \sin^2(\omega t_{mn})\} \\
- \quad & \cos(\psi) a_m [\sum_{n=0}^{N-1} x_m[n](e^{-jn\omega T} e^{-j(kM+m)N\omega T} + e^{jn\omega T} e^{j(kM+m)N\omega T})] \\
- \quad & j\cos(\psi) b_m [\sum_{n=0}^{N-1} x_m[n](e^{-jn\omega T} e^{-j(kM+m)N\omega T} - e^{jn\omega T} e^{j(kM+m)N\omega T})] \\
- \quad & \sin(\psi) a_m [\sum_{n=0}^{N-1} y_m[n](e^{-jn\omega T} e^{-j(kM+m)N\omega T} + e^{jn\omega T} e^{j(kM+m)N\omega T})] \\
- \quad & j\sin(\psi) b_m [\sum_{n=0}^{N-1} y_m[n](e^{-jn\omega T} e^{-j(kM+m)N\omega T} - e^{jn\omega T} e^{j(kM+m)N\omega T})]
\end{aligned}
$$

By the definition of Discrete Fourier Transform(DFT),

$$
\begin{aligned}
X_m(\omega) &= \sum_{n=0}^{N-1} x_m[n] e^{-jn\omega T} \\
Y_m(\omega) &= \sum_{n=0}^{N-1} y_m[n] e^{-jn\omega T}
\end{aligned}
\tag{6.2.7}
$$

and properties of real data's DFT

$$
\begin{aligned}
X_m(-\omega) e^{j(kM+m)N\omega T} &= \{X_m(\omega) e^{-j(kM+m)N\omega T}\}^* \\
Y_m(-\omega) e^{j(kM+m)N\omega T} &= \{Y_m(\omega) e^{-j(kM+m)N\omega T}\}^*
\end{aligned}
\tag{6.2.8}
$$

and simplified denotation

$$
\tilde{X}_m(\omega) = X_m(\omega) e^{-j(kM+m)N\omega T}, \qquad \tilde{Y}_m(\omega) = Y_m(\omega) e^{-j(kM+m)N\omega T}
\tag{6.2.9}
$$

in connection with approximation

$$
\begin{aligned}
\sum_{n=0}^{N-1} \cos^2(\omega t_{mn}) &\approx \frac{N}{2} \\
\sum_{n=0}^{N-1} \sin^2(\omega t_{mn}) &\approx \frac{N}{2} \\
\sum_{n=0}^{N-1} \sin(2\omega t_{mn}) &\approx 0
\end{aligned}
\tag{6.2.10}
$$

We can simplify γ_m^2 as

$$\begin{aligned}\gamma_m^2 &= \sum_{n=0}^{N-1} x_m[n]^2 + \sum_{n=0}^{N-1} y_m[n]^2 + \frac{N}{2}(a_m^2 + b_m^2) \\ &- \cos(\psi)a_m \cdot 2Re[\tilde{X}_m(\omega)] + \cos(\psi)b_m \cdot 2Im[\tilde{X}_m(\omega)] \\ &- \sin(\psi)a_m \cdot 2Re[\tilde{Y}_m(\omega)] + \sin(\psi)b_m \cdot 2Im[\tilde{Y}_m(\omega)]\end{aligned} \tag{6.2.11}$$

To get solutions that make the square error γ^2 minimal, take first derivative with a_m, b_m, ψ separately. Since a_m, b_m are independent with each other, then

$$\begin{aligned}\frac{\partial\gamma^2}{\partial a_m} &= \frac{\partial\gamma_m^2}{\partial a_m} = Na_m - 2\cos(\psi)Re[\tilde{X}_m(\omega)] - 2sin(\psi)Re[\tilde{Y}_m(\omega)] = 0 \\ \frac{\partial\gamma^2}{\partial b_m} &= \frac{\partial\gamma_m^2}{\partial b_m} = Nb_m + 2\cos(\psi)Im[\tilde{X}_m(\omega)] + 2sin(\psi)Im[\tilde{Y}_m(\omega)] = 0\end{aligned} \tag{6.2.12}$$

$$\begin{aligned}\frac{\partial\gamma^2}{\partial\psi} &= \sum_{m=0}^{M-1} \frac{\partial\gamma_m^2}{\partial\psi} \\ \frac{\partial\gamma_m^2}{\partial\psi} &= sin(\psi)\{a_m \cdot 2Re[\tilde{X}_m(\omega)] - b_m \cdot 2Im[\tilde{X}_m(\omega)]\} \\ &\quad - \cos(\psi)\{a_m \cdot 2Re[\tilde{Y}_m(\omega)] - b_m \cdot 2Im[\tilde{Y}_m(\omega)]\}\end{aligned} \tag{6.2.13}$$

From Eq.6.2.12 we can get

$$\begin{aligned}\hat{a}_m &= \frac{2}{N}\{\cos(\psi)Re[\tilde{X}_m(\omega)] + sin(\psi)Re[\tilde{Y}_m(\omega)]\} \\ \hat{b}_m &= -\frac{2}{N}\{\cos(\psi)Im[\tilde{X}_m(\omega)] + sin(\psi)Im[\tilde{Y}_m(\omega)]\}\end{aligned} \tag{6.2.14}$$

Substitute the above result into Eq.6.2.13, and with

$$Re[\tilde{X}_m(\omega)]Re[\tilde{Y}_m(\omega)] + Im[\tilde{X}_m(\omega)]Im[\tilde{Y}_m(\omega)] = Re[\tilde{X}_m(\omega)\tilde{Y}_m^*(\omega)] \tag{6.2.15}$$

we can get

$$\begin{aligned}\frac{\partial\gamma_m^2}{\partial\psi} &= \frac{4}{N}\sin(\psi)\cos(\psi)(\|\tilde{X}_m(\omega)\|^2 - \|\tilde{Y}_m(\omega)\|^2) \\ &\quad -\frac{4}{N}(\cos^2(\psi) - \sin^2(\psi))Re[\tilde{X}_m(\omega)\tilde{Y}_m^*(\omega)]\}\end{aligned} \tag{6.2.16}$$

Then

$$\frac{\partial \gamma^2}{\partial \psi} = \frac{2}{N}\sin(2\psi)\sum_{m=0}^{M-1}[\|\tilde{X}_m(\omega)\|^2 - \|\tilde{Y}_m(\omega)\|^2] - \frac{4}{N}\cos(2\psi)\sum_{m=0}^{M-1} Re[\tilde{X}_m(\omega)\tilde{Y}_m^*(\omega)] \tag{6.2.17}$$

Or express it as (assume $\psi \neq (2N+1)\pi/4$)

$$\tan(2\psi) = \frac{2\sum_{m=0}^{M-1} Re[\tilde{X}_m(\omega)\tilde{Y}_m^*(\omega)]}{\sum_{m=0}^{M-1}[\|\tilde{X}_m(\omega)\|^2 - \|\tilde{Y}_m(\omega)\|^2]} \tag{6.2.18}$$

Then the solution is

$$\psi = \frac{1}{2}\arctan\{\frac{2\sum_{m=0}^{M-1} Re[\tilde{X}_m(\omega)\tilde{Y}_m^*(\omega)]}{\sum_{m=0}^{M-1}[\|\tilde{X}_m(\omega)\|^2 - \|\tilde{Y}_m(\omega)\|^2]}\} \tag{6.2.19}$$

For square error

$$\begin{aligned}\gamma_m^2 = & \sum_{n=0}^{N-1} x_m[n]^2 + \sum_{n=0}^{N-1} y_m[n]^2 - \frac{N}{2}(\hat{a}_m^2 + \hat{b}_m^2) \\ = & \sum_{n=0}^{N-1} x_m[n]^2 + \sum_{n=0}^{N-1} y_m[n]^2 \\ & -\frac{2}{N}\{\cos^2(\psi)\|\tilde{X}_m(\omega)\|^2 + \sin^2(\psi)\|\tilde{Y}_m(\omega)\|^2 + sin(2\psi)Re[\tilde{X}_m(\omega)\tilde{Y}_m^*(\omega)]\}\end{aligned} \tag{6.2.20}$$

We can see, for each value of ω, there is a corresponding ψ. For γ_m^2, let's define the part contain function of ψ as $\beta_m(\omega,\psi)$.With the relation in Eq.6.2.16, $\beta_m(\omega,\psi)$ can be more simplified as

$$\begin{aligned}\gamma_m^2 = & \sum_{n=0}^{N-1} x_m[n]^2 + \sum_{n=0}^{N-1} y_m[n]^2 - \beta_m(\omega,\psi) \\ \beta_m(\omega,\psi) = & \frac{1}{N}\{\|\tilde{X}_m(\omega)\|^2 + \|\tilde{Y}_m(\omega)\|^2 + \sec(2\psi)[\|\tilde{X}_m(\omega)\|^2 - \|\tilde{Y}_m(\omega)\|^2]\}\end{aligned} \tag{6.2.21}$$

If ψ is known, for determinate M and N, the value of γ^2 only depends on ω, thus the maximum likelihood estimate of ω :

$$\hat{\omega} = \max_{\omega}\sum_{m=0}^{M-1}\beta_m(\omega,\psi) \tag{6.2.22}$$

Notice that, the estimation of ω contains ψ, and estimation of ψ also contains ω.

Finally, we summarize all the parameter estimations under H_1 hypothesis:

$$\begin{aligned}
\hat{\omega} &= \max_{\omega} \sum_{m=0}^{M-1} \beta_m(\omega, \psi) \qquad (6.2.23)\\
\beta_m(\omega,\psi) &= \frac{1}{N}\{\|\tilde{X}_m(\omega)\|^2 + \|\tilde{Y}_m(\omega)\|^2 + \csc(2\psi)[\|\tilde{X}_m(\omega)\|^2 - \|\tilde{Y}_m(\omega)\|^2]\}\\
\hat{\psi} &= \frac{1}{2}\arctan\{\frac{2\sum_{m=0}^{M-1} Re[\tilde{X}_m(\omega)\tilde{Y}_m^*(\omega)]}{\sum_{m=0}^{M-1}[\|\tilde{X}_m(\omega)\|^2 - \|\tilde{Y}_m(\omega)\|^2]}\}\\
\hat{a}_m &= \frac{2}{N}\{\cos(\psi)Re[\tilde{X}_m(\hat{\omega})] + sin(\psi)Re[\tilde{Y}_m(\hat{\omega})]\}\\
\hat{b}_m &= -\frac{2}{N}\{\cos(\psi)Im[\tilde{X}_m(\hat{\omega})] + sin(\psi)Im[\tilde{Y}_m(\hat{\omega})]\}\\
\hat{\sigma_1^2} &= \frac{1}{MN}\{\sum_{m=0}^{M-1}\sum_{n=0}^{N-1}(x_m^2[n] + y_m^2[n]) - \sum_{m=0}^{M-1}\beta_m(\hat{\omega},\hat{\psi})\}\\
f_{\Theta}(\mathbf{x},\mathbf{y};H_1) &= (2\pi\hat{\sigma_1^2})^{-MN}\exp(-MN)
\end{aligned}$$

Now we can represent the likelihood ratio for hypothesis H_1 and H_0 as

$$L_G(\mathbf{x},\mathbf{y}) = \frac{f_{\Theta}(\mathbf{x},\mathbf{y};H_1)}{f_{\Theta}(\mathbf{x},\mathbf{y};H_0)} = (\frac{\hat{\sigma_1^2}}{\hat{\sigma_0^2}})^{-MN} \qquad (6.2.24)$$

Since M and N are known, for each window, the test statistics can also be represented as

$$t_G(\mathbf{x},\mathbf{y}) = \frac{\sum_{m=0}^{M-1}\sum_{n=0}^{N-1}(x_m^2[n] + y_m^2[n])}{\sum_{m=0}^{M-1}\sum_{n=0}^{N-1}(x_m^2[n] + y_m^2[n]) - \sum_{m=0}^{M-1}\|\beta_m(\hat{\omega})\|^2} \qquad (6.2.25)$$

To get test statistics, we only need to evaluate the power of received signal, and search the peak of modified averaged PSD. We can also substitute Goertzel algorithm with FFT. Although it's more complex to get modified averaged PSD, the detector is still based on GLRT and FFT. Therefore, its computation is not much heavier. On the other hand, complex data model don't require SVD combination. In conclusion, for complex data model, the detection proposal based on FFT-GLRT is still fast and simple enough.

6.3 Detection performance analysis

6.3.1 Definition of P_A, P_D and ROC

To evaluate the performance of the proposed detector resulting from the Pearson-Pearson detection theory, we can employ the receiver operating characteristic (ROC) analysis. It provides an effective tool to measure the trade-off between the detection power and false-alarm probability.

Let's first give a definition for detection power and false alarm probability. In a hypothesis test, there are two types of errors. A type I error occurs when the null hypothesis is rejected when it is in fact true; that is, H_0 is wrongly rejected. A type II error occurs when the null hypothesis H_0, is accepted when it is in fact false. For any given set of data, type I and type II errors are inversely related; the smaller the risk of one, the higher the risk of the other. A type I error is often considered to be more serious, and therefore more important to avoid, than a type II error. This probability of a type I error is named as False Alarm Probability, and can be precisely computed as

$$P\{\texttt{type I error}\} = \alpha = P_{FA} \tag{6.3.1}$$

If we do not reject the null hypothesis, it may still be false (a type II error) as the sample may not be big enough to identify the falseness of the null hypothesis (especially if the truth is very close to hypothesis). The probability of a type II error is generally unknown, but is symbolized by β and written as

$$P\{\texttt{type II error}\} = \beta \tag{6.3.2}$$

The power of a statistical hypothesis test measures the test's ability to reject the null hypothesis when it is actually false - that is, to make a correct decision. It is calculated by subtracting the probability of a type II error from 1, usually denoted by P_D and expressed

as:

$$Power = 1 - P\{\texttt{type II error}\} = 1 - \beta = P_D \tag{6.3.3}$$

The maximum power a test can have is 1, the minimum is 0. For a given false alarm probability P_{FA}, we hope the detection power P_D as high as possible.

6.3.2 Apply thresholds and get P_D for a given P_{FA}

To examine the FFT-GLRT-based detection proposals for real and complex models, we simulate with real time data to get ROC curves. We totally use 16 measurements. Each measurement lasts for 5 minutes. All the measurements use two antennas as receiver, which are fixed horizontally about 0.5 meters away from the subjects, with DOA from 0 to 30 degree. A single subject sits in front of the antenna arrays. After getting the GLRT statistics of all 16 measurements, we apply the same threshold to all the statistics, and conclude a pair of(P_{FA}, P_D).

Fig.6.1 and Fig.6.2 shows how to apply a fitting threshold for real data model GLRT statistics. The figures show and compare the resulting P_D with a given $P_{FA} = 0.1$. We can see, since reference signal has high SNR, the resulting detection probability is as high as $P_D = 1$. From this, our detectors can be verified successful for high SNR. However, for wireless data, the P_D value will be different, the P_D(=0.83281) for $subwindow = 24s$ is obviously higher than that of $subwindow = 32s$, ($P_D = 0.66667$). The detection performance seems highly related to the subwindow length and order (number of subwindows in a window).

6.3.3 Simulation results and ROC curves

Although we assume subwindow length and order are known in our modified model, we actually don't know what value is the optimal for these two parameters. To give

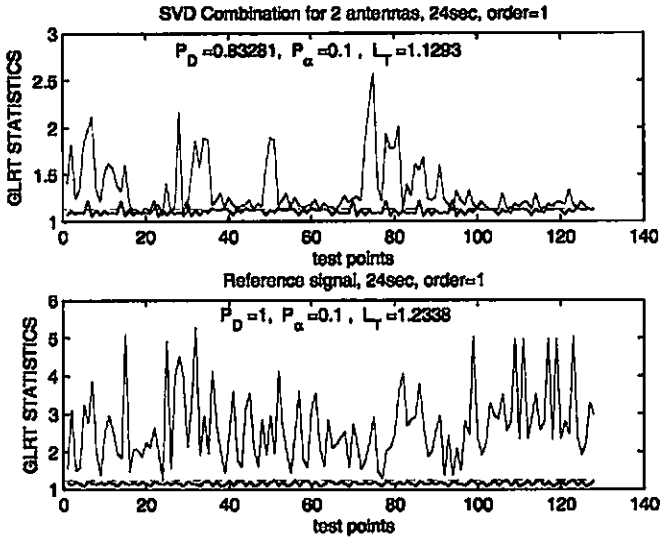

Figure 6.1: Read data model with SVD combination, P_D under a given P_{FA}, window = 24s

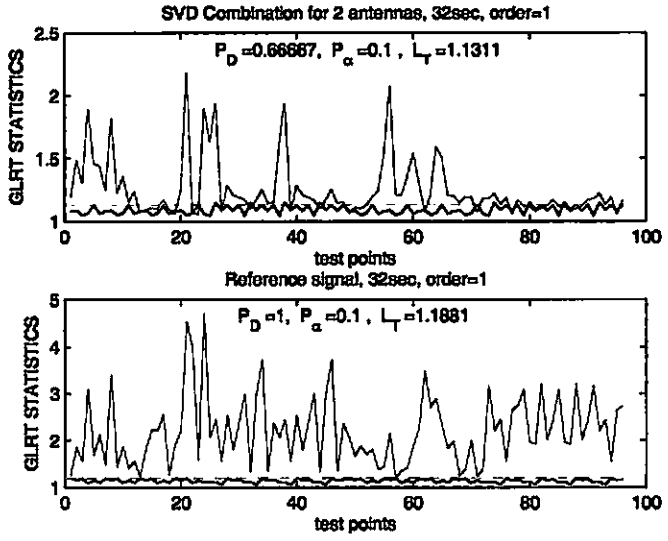

Figure 6.2: Reference data, P_D under a given P_{FA}, window = 24s

some recommendation, we run a large amount of simulation to explore good values for them. The criterion is to compare ROC curves under different parameters.

The following ROC curves are produced by the 16 measurements of wireless data. Each measurement contains one single person case dataset and one nobody case dataset. Simulation is proceeded with various values of window length, subwindow length and order, with aim to discover the best values for these parameters. Although the ROC gives P_D for $0 \leq P_{FA} \leq 1$, in real life, we only interested in the P_D for small value of P_{FA}. Otherwise, it's useless to examine the detector's performance when the probability of first type error is as high as 30 percent or more! Thus, in this section, we examine ROC curves with emphasis on reasonable range $0 \leq P_{FA} \leq 0.3$.

From simulation, I find that under window = 24s or 32s, most of the dataset can achieve a reasonable high detection probability. For each window length, we'll compare the results versus different orders and subwindows.

Let's first examine real model data with SVD combination of 4 channels; the results are shown in Fig.6.3 and Fig.6.4. It can be observed that, for window = 24s, $(subwindow = 3s, order = 8)$ and $(subwindow = 4s, order = 6)$ are the best. For window = 32s, $(subwindow = 4s, order = 8)$ and $(subwindow = 8s, order = 4)$ outperform others. We can see, increasing number of subwindow is really helpful, however, increasing too much is helpless. We must select fitting values for both subwindow and order.

To refine our selection, we plot the curves for all these recommended values into one figure, Fig.6.5. Their resulting performances are comparable. For $0.1 \leq P_{FA} \leq 0.2$, it is shown experimentally that $(subwindow = 3s, order = 8)$ is optimal, which can provide P_D as high as more than 0.9. While for small value $P_{FA} \leq 0.1$, it implies that $(subwindow = 8s, order = 4)$ can keep a satisfactory P_D, which can remain as high as 0.85.

For these two window lengths, I think these parameter pairs are highly recommended: (subwindow, order) = (3s, 8), (4s,6), (4s,8), (8s,4). These recommendations give us a good reference. However, there is no assurance of optimality. We still need more measurements to verify them and find the ideal window length, subwindow length and order.

For complex model data, we examine ROC curves for 2 antennas separately. Simulation was performed with the recommended parameter pairs. Fig.6.6 is for antenna 2, and Fig.6.6 is for antenna 1. Fig.6.10 and Fig.6.10 separately compare their performances with that of real model with SVD combination. Generally , complex model results better than real model with SVD combination. This is attribute to that complex model exploits more information, the DOA and distance, to detect and estimate. We can see, Antenna 2's complex model results are always better than that of real model with SVD combination. However, antenna 1 cannot assure these. Further, Fig.6.10 compare the performances for two antennas. We can find that antenna 2 is always better than antenna 1.

The difference may due to hardware IQ imbalance. For example, channel I and Q have slightly different magnitudes., or they don't have ideal 90 degree phase difference. To check IQ imbalance, we examine the datasets when nobody was present. We have 16 measurements, each of which has a nobody case data. We find that, for all the nobody case datasets, two antennas show different IQ plots as Fig.6.11: antenna 2 always show the same near circle clouds, while antenna 1 always show the same ellipse clouds with a certain angle. If an antenna has no IQ imbalance, then its internal thermal noise will have a IQ constellation with a perfect circle cloud shape, while all the samples are uniformly distributed inside or on the circle. Therefore, we can conclude, antenna 1 has much much more severe IQ imbalance: ellipse cloud is attribute to different magnitudes in IQ; certain angle is due to IQ phase difference is not 90 degree. Although complex model should work better than real model, under IQ imbalance, SVD combination can correct the imbalance in a sense, thus, sometimes their performance comparison results appear on the contrary.

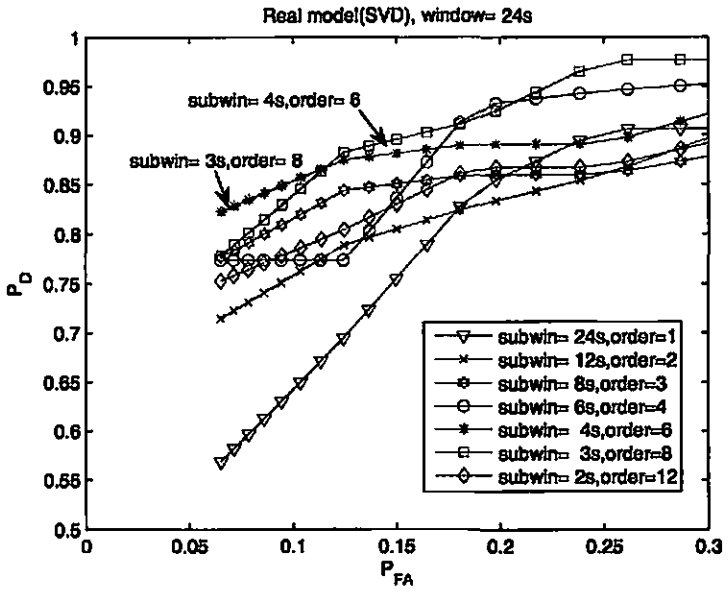

Figure 6.3: ROC: Simulation for window=24s, real model with SVD combination

To compensate IQ imbalance, the exact IQ magnitude ratio and phase difference should be examined. However, it's hard to extract these information from the measured datasets. We have to do some experiment with pure sinusoids to find it. This problem will be solved later.

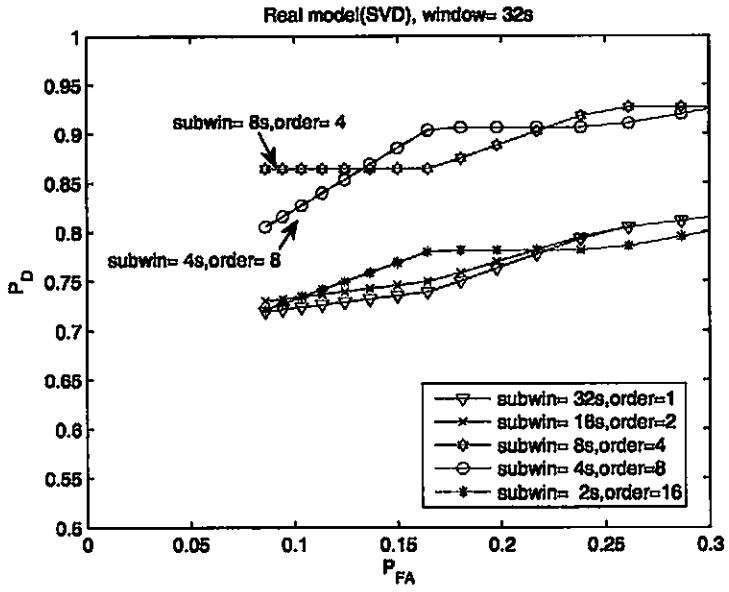

Figure 6.4: ROC: Simulation for window=32s, real model with SVD combination

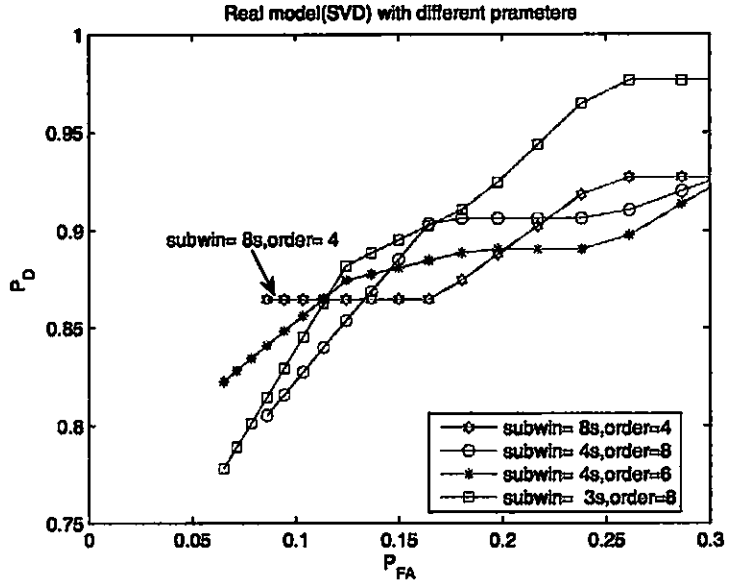

Figure 6.5: ROCs for real model with SVD combination versus different parameters

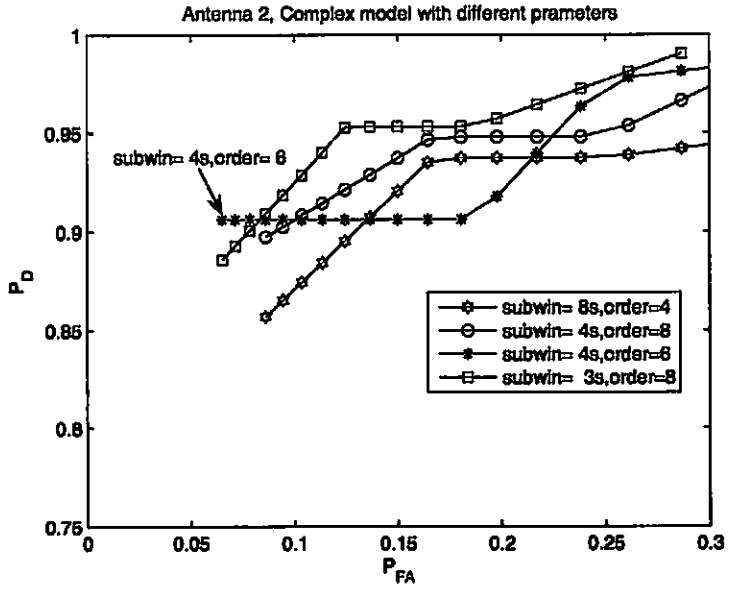

Figure 6.6: ROCs of Antenna 2 for complex model versus different parameters

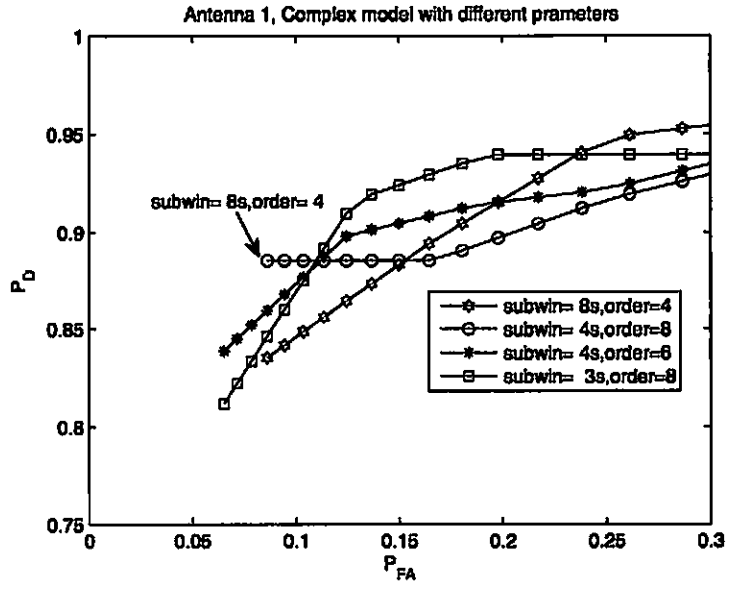

Figure 6.7: ROCs of Antenna 1 for complex model versus different parameters

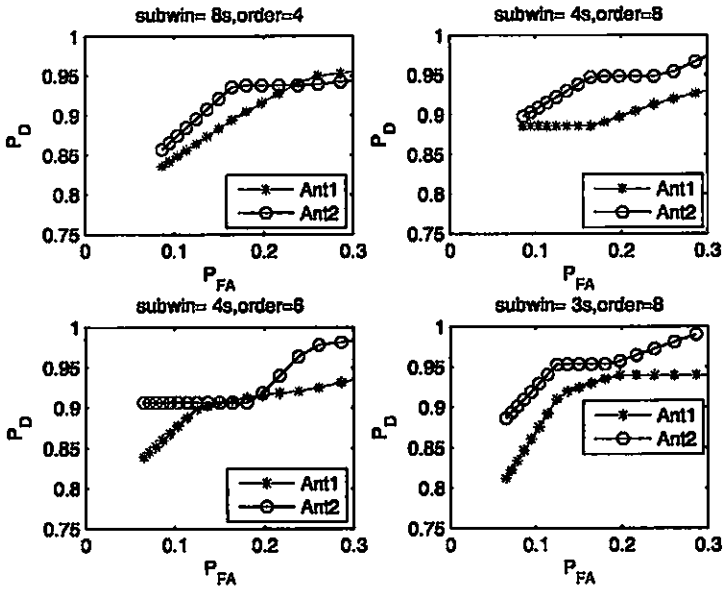

Figure 6.8: ROC comparison: real model (SVD) versus complex model, antenna 2

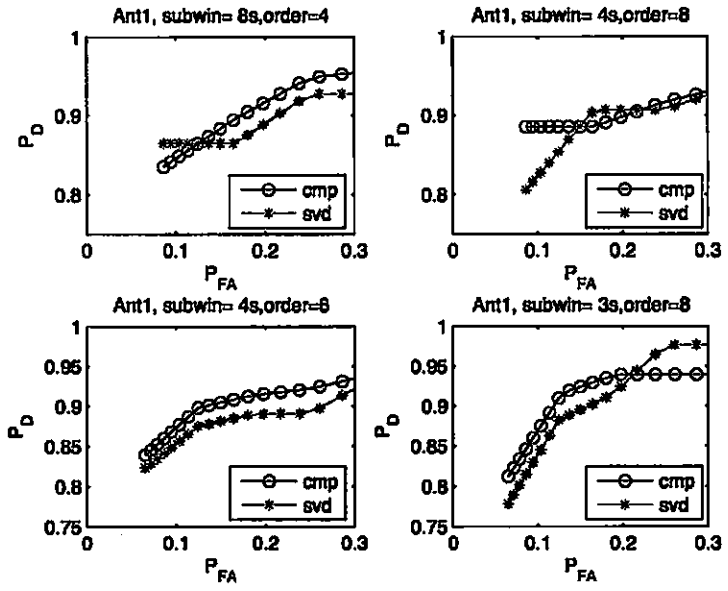

Figure 6.9: ROC comparison: real model (SVD) versus complex model, antenna 1

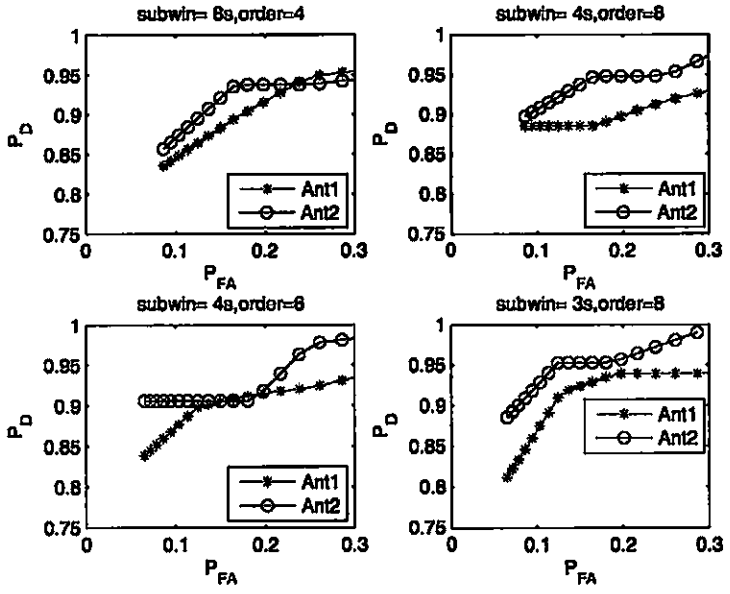

Figure 6.10: ROC comparison for complex model: antenna 2 versus antenna 1

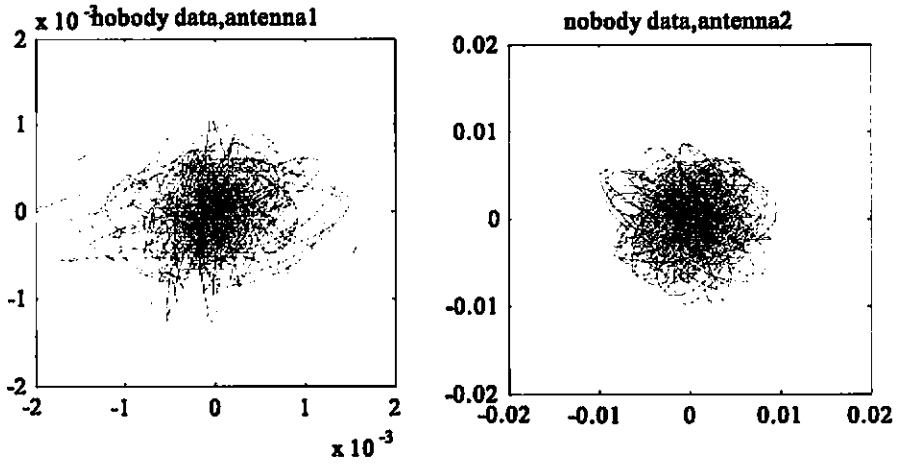

Figure 6.11: IQ Plot of noise at 2 antennas

Chapter 7

Further Research Ideas

When 2 subjects are present, samples of the received data cannot be expressed in a linear combination of FFT of subwindow data any more, because there are cross terms of 2 subjects' heartbeats. Thus it's not easy to get MLE of the frequencies of two subjects as fast FFT-GLRT-based proposal does.

In such cases, a source separation technique that exploits, for example, Constant Modulus Algorithm(CMA)[31] can be used to sort out the individual signals. In a second step, the FFT-GLRT-based single subject detection proposal can be also utilized for each separated signal, therefore to determine whether there are 2 targets or not. Since an other graduate student is researching about this problem, it won't be discussed in this thesis.

Another promising method is based on MUltiple SIgnal Classification (MUSIC) algorithm. The MUSIC algorithm proposed by Schmidt in 1979 [35][36] is a high-resolution multiple signal classification technique based on exploiting the eigenstructure of the input covariance matrix. MUSIC algorithm can provides information about the number of incident signals, Direction-Of-Arrival (DOA) of each signal, strengths and cross correlation between incident signals, noise power, etc. Hence, it can detect the number of subjects and locate them. While the MUSIC algorithm provides very high resolution, it requires very precise and accurate array calibration. Various modifications to the MUSIC algorithm

have been proposed to increase its resolution performance and decrease the computational complexity. One such improvement is the ROOT-MUSIC algorithm developed by Barabell [37], which is based on polynomial rooting and provides higher resolution. Barabell [37] showed through simulations that the ROOT-MUSIC algorithm has better resolution than the classical MUSIC algorithm, especially at low SNR conditions [32][34].

Chapter 8

Conclusions

In this thesis, we have investigated how to detect heartbeats by taking advantage of Doppler shift. It's a difficult problem because heartbeat is a nonstationary time-variant heartbeat signal, which imposes an adverse condition to measurement and detection.

To analyze and design effective detection schemes, we derived the received baseband signal model. After removing the useless DC offset in I and Q separately, the received baseband signal can be expressed as

$$\begin{aligned} I &\approx C\cos(\psi)x(t) + Re\{w(t)\} \\ Q &\approx C\sin(\psi)x(t) + Im\{w(t)\} \end{aligned} \tag{8.0.4}$$

ψ depends on the distance and DOA between subjects and antenna. And C is constant depending on each subject. Based on heartbeat properties in time and frequency, a simplification is made to treat heartbeat as a sinusoid like signal with unknown frequency and variant phase. Within each detection window, it is modeled as a sinusoid $x(t) = A\cos(\omega t + \theta)$, with constant frequency, but staircase jumpily variant phase and magnitude from subwindow to subwindow.

Under the above signal model, the detection problem is equivalent to find how many such sinusoids exist. Although heartbeat signals are very weak and complicate, it's

shown that, by using *General Likelihood Ratio Test (GLRT)*, it is possible to distinguish among the presence of 2, 1, or 0 subjects, even with single antenna. However, for some datasets, the detection performance is not satisfactory. We find window structure is critical to performance. More antennas can also improve detection probability.

Since the heartbeat signal embedded in inphase and quadrature phase data in different ways, we can use real signal (I or Q) or complex signal to perform detection, both based on GLRT. For real data model, to achieve good and stable performance for all measurements, we can apply SVD combination method to enhance SNR in order to achieve better performance. For complex data model, we could possibly get improvement by taking into account the embedded spatial information.

We mainly investigate detection for 1/0 subject, and novel fast FFT-GLRT-based algorithms for both real and complex data models are proposed. In these algorithms, MLE of the heartbeat frequency is equivalent to evaluate the peak of averaged FFT; and the test statistics can be simply expressed in terms of input signal's power and the mentioned peak. For simplicity, we can substitute Goertzel algorithm with FFT. Simulation results are compared and analyzed. The following window structures are recommended: $(subwindow, order) = (4s, 8), (8s, 4), (4s, 6), (3s, 8)$. For complex model, with these window structures, for $P_{FA} \leq 0.1$ we can achieve high $P_D \geq 0.85$. Generally , complex model results better than real model with SVD combination. Even one antenna's complex data can outperform 2 antennas' SVD combination under real model. This is attribute to that complex model exploits more information, the DOA and distance, to detect and estimate. However, IQ imbalance will decrease the performance of complex model data. Before detection, we must compensate IQ imbalance beforehand.

In conclusion, the main contributions of this thesis include: 1)proposed an effective time-varying sinusoid model for heartbeat; 2)derived fast FFT-GLRT-based detectors for Real and complex data for signal subject detection; 3) recommended some window

structures for reference. The future work will focus on design simple but efficient detectors for 2-target present case.

Bibliography

[1] Boric-Lubecke, O., Droitcour, A.D., Lubecke, V.M., Jenshan Lin, Kovacs, G.T.A. "Wireless IC Doppler radars for sensing of heart and respiration activity ," *Telecommunications in Modern Satellite, Cable and Broadcasting Service, 2003. TELSIKS 2003. 6th International Conference*, on Volume 1, 1-3 Oct. 2003. Page(s):337 -344 vol.1

[2] J. Lin, "Applying telecommunication technology to health-care delively," *IEEE Engineering in Medicine and Biology*, vol. 18, no. 4, pp. 28-3 1, 1999.

[3] K. Simizu, "elemedicine by mobile communication," *IEEE Engineering in Medicine and Biology*, vol. 18, no. 4, pp. 32-44, 1999.

[4] J. C. Lin, "Non-invasive microwave measurement of respiration," *Proc. of IEEE*, vol. 63, pp. 1530, 1979.

[5] J. C. Lin, J. Kiemicki, M. Kiemich, P. B. Wollschaeger, "Microwave apexcardiography," *IEEE Tran. Microwave Theory and Technique*, vol. 27, pp. 618-620, 1979.

[6] V. M. Lubecke, 0. Boric-Lubecke, G. Awater, P.-W. Ong, P. L. Gammel, R.-H. Yan, and J. C. Lin, "Remote sensing of vital signs with telecommunications signals," *World Congress on Medical Physics and Biomedical Engineering*, Chicago IL, July 2000.

[7] Olga Boric-Lubecke, Victor M. Lubeckel, Anders Host-Madsen1, Dragan Samardzija , and Ken Cheung, "Doppler Radar Sensing of Multiple Subjects in Single and

Multiple Antenna Systems," *Telecommunications in Modern Satellite, Cable and Broadcasting Services, 2005. 7th International Conference* on Sept. 2005, page(s): 7-11 vol. 1

[8] J. C. Lin, "Microwave sensing of physiological movement and volume change: a review," *Bioelectromagnetics*, vol. 13, pp. 557-565, 1992.

[9] K. M. Chen, D. Mirsa, H. Wang, H. R. Chuang, E. Postow, " An X-band microwave life detection system," *IEEE Transactions of Biomedical Eng.*, vol. 33, pp. 697-70, 1986.

[10] Lin-Sen Pon; Gephart, K.; Mingui Sun; Sclabassi,R.J., "Analysis of heart rate changes associated with ictal activity," *Engineering in Medicine and Biology Society, 2000. Proceedings of the 22nd Annual International Conference of the IEEE*, Volume 1, Page(s):68 - 70 vol.1, 23-28 July 2000.

[11] Task Force (1996). "Heart rate variability: standards of measurement, physiological interpretation and clinical use ," *Task Force of the European Society of Cardiology and the North American Society of Pacing and Electrophysiology* , Circulation 93: 1043-1065

[12] M.H. Asyali, "Discrimination Power of Long-Term Heart Rate Variability Measures," *Proceedings of the 25th Annual International Conference of the IEEE Engineering in Medicine and Biology Society*, Cancun, September 17-21, 2003.

[13] Pilgram B and Kaplan DT, "Non-stationary and 1/f noise characteristics in heart rate". *Am. J. Physiol. Regul. Integr. Comp. Physiol.* 1999. 276 R1C9

[14] GB Moody, "Spectral Analysis of Heart Rate Without Resampling", *Computers in Cardiology*, 1993, vol. 20, pp. 715-718. Harvard-M.I.T. Division of Health Sciences and Technology, Cambridge, MA, USA.

[15] C.-K. Peng, J. Mietus, JM Hausdorff, S. Havlin, HE Stanley and AL Goldberger, "Long-range anticorrelations and non-gaussian behaviour of the heartbeat". *Phys. Rev. Lett.* 70: 1343 C 1346, 1993.

[16] S. S. Abeysekera, U. R. Abeyratne and S. B. Goh, " Spectral information changes in obtaining heart rate variability from tachometer R-R interval signals", *18th Southern Biomedical Engineering Conference*, (Abstract in: Critical Reviews in Biomedical Engineering, vol. 26, no. 5-6, pp. 325-326, 1998), South Carolina, USA, May 1999.

[17] Mitov V, " Spectral analysis of heart rate variability using the integral pulse frequency modulation model". *Med Biol Eng Comput 2001.*

[18] Patrick E. McSharry, Gari Clifford, Lionel Tarassenko and Leonard A. Smith. " A dynamical model for generating synthetic electrocardiogram signals", *IEEE Transactions on Biomedical Engineering*, 50(3):289-294; March 2003.

[19] S.M. Kay, *Fundamentals of statistical signal processing*, Vol. 2, Prentice Hall, 1998.

[20] L. L. Scharf, *Statistical Signal Processing: Detection, Estimation, and Time Series Analysis*. Reading (MA), USA: Addison-Wesley Publishing Company, Inc., 1991.

[21] John G. Proakis and Dimitris G. Monoakis. *Digital Signal Processing - Principles, Algorithms, and Applications*. Prentice-Hall, 3 edition, 1996.

[22] Tufts D., Kumaresan R., " Estimation of frequencies of multiple sinusoids: making linear prediction perform like maximum likelihood", *Proc. IEEE*, Vol. 70, no. 9, pp. 975-989, Sept. 1982

[23] Stoica P., Soderstroni T., " Asymptotic prop- erties of the high order Yule Walker estimates of sinusoidal frequencies", *IEEE Trans. Acoustic, Speech and Signal Proc.*, Vol. 37, no. 11, pp. 1721- 1734, NOV. 1989

[24] D. Rife and R. Boorstyn, " Single-tone parameter estimation from discrete- time observations," *IEEE Trans. Inform. Theory,* vol. IT-20, pp. 591C598, Sept. 1974.

[25] JJ Fuchs, RI IRISA, " Estimating the Number of Sinusoids in Additive White Noise". *IEEE Trans. on Acoustics, Speech, and Signal. Processing*, ASSP-36(12):1846-1853, December 1988.

[26] H. Akaike, " A new look at the statistical model identifi- cation," *IEEE Trans. Automat. Contr.*, vol. AC-19, pp. 716-723, Oct.1974.

[27] J. Rissanen, " Modeling by shortest data description," *Automica.* vol. 14, pp. 465471, May 1978.

[28] J. Q. Zhang, S. J. Ovaska, and X. Z. Gao, " An eigenvalue residuum-based criterion for detection of the number of sinusoids in white Gaussian noise," *IEEE Southeastcon99*, Lexington, Kentucky, 1999.

[29] L. L. Scharf, *Statistical Signal Processing: Detection, Estimation, and Time Series Analysis*. Reading (MA), USA: Addison-Wesley Publishing Company, Inc., 1991.

[30] Phornphop Naiyanetr, Pornpimol Charoentong, and Warakorn Charoensuk, " ECG System With Heart Rate Variability Application," *IEEE TENCON 2004*, 21-24 November 2004, Lotus Hotel Pang Suan Kaew, Chiang Mai, Thailand, Conference Proceedings; pp.133.

[31] Papadias, C.B.; Paulraj, A.J.; " A constant modulus algorithm for multiuser signal separation in presence of delay spread using antenna arrays", *Signal Processing Letters*, IEEE Volume 4, Issue 6, June 1997 Page(s):178 - 181.

[32] Joseph Liberti, Theodore S. Rappaport, *Smart Antennas for Wireless Communications: IS-95 and Third Generation CDMA Applications*, Edition: 1st, Prentice Hall, 1999. Page(s):253 - 284.

[33] S. Haykin, *Unsupervised adaptive filtering, volume 1: blind source separation*, John Wiley and Sons, Inc., 2000.

[34] Harry L. Van Trees, *Detection, Estimation, and Modulation Theory, Part IV, Optimum Array Processing*, John Wiley and Sons, 2002.

[35] R. O. Schmidt, " Multiple emitter location and signal parameter estimation", *Proceedings RADC, Spectral Estimation Workshop*, Rome, NY, (243-258) 1979.

[36] R.O. Schmidt, " Multiple emitter location and signal parameter estimation," *IEEE Trans. Antennas Propag.*, vol.34, no.3, pp.276C280, 1986.

[37] A. Barabell, " Improving the resolution performance of eigenstructure-based direction-finding algorithms", *Proceedings of the ICASSP'83*, 1983, pp. 336-339.

[38] A. Belouchrani, K. A. Meraim, J.-F. Cardoso, and E. Moulines, " A blind source separation technique using second order statistics," *IEEE Trans. Signal Processing*, vol. 45, pp. 434-444, Feb. 1997.

[39] A. Belouchrani and M. G. Amin, " Time-frequency MUSIC," *IEEE Signal Processing Lett.*, vol. 6, pp. 109-110, May 1999.

[40] Bousbia-Salah, A.; Belouchrani, A.; Cichocki, A.; " Application of time-frequency distributions to the independent component analysis of ECG signals". *Signal Processing and its Applications, Sixth International, Symposium* on. 2001. vol.1, pp.238 - 241, Aug. 2001.